Interim Report 63-1

THE ENERGY BUDGET AT THE EARTH'S SURFACE

Edgar R. Lemon, USDA

Research Investigations Leader
Micro-climate Investigations

Contribution by:

Zenbei Uchijima and James L. Wright

An Experimental Study of Air Flow in a Corn Plant-Air Layer

RESEARCH REPORT NO. 367

Northeast Branch
Soil and Water Conservation Research Division
Agricultural Research Service
U. S. Department of Agriculture

In Cooperation with

N. Y. S. College of Agriculture
Cornell University
Ithaca, New York

for

Meteorology Department
U. S. Army Electronics Research & Development Activity
Fort Huachuca, Arizona

JULY 1963

Bailey Hall, Ithaca, N. Y.

INTERIM REPORT 63-1

AN EXPERIMENTAL STUDY OF AIR FLOW IN A CORN PLANT-AIR LAYER

by

Zenbei Uchijima and James L. Wright

DA TASK 1-A-0-11001-B-021-08

under

Cross Service Order No. 2-63

for

Meteorology Department
U. S. Army
Electronics Research & Development Activity
Fort Huachuca, Arizona

U. S. Department of Agriculture
Research Report No. 367

July, 1963

Bailey Hall, Ithaca, N. Y.

AN EXPERIMENTAL STUDY OF AIR FLOW IN A CORN PLANT-AIR LAYER[1/]

by

Zenbei Uchijima and James L. Wright[2/]

Northeast Branch
Soil and Water Conservation Research Division
Agricultural Research Service
U. S. Department of Agriculture
Ithaca, New York

ABSTRACT

Data are processed to provide the characteristics of air flow in the corn plant-air layer. From wind velocity measurements at 130, 110, 90, and 50-cm. heights, the shearing stress, friction velocity, exchange coefficient, and mixing length are calculated for the respective heights. The data indicate that the height dependence of shearing stress, friction velocity, and exchange coefficient can be expressed as an exponential function of height. Near the ground, the mixing length increased linearly with increment of height above the ground (constant of proportionality = 0.4).

1/ Contribution from the Soil and Water Conservation Research Division, Agricultural Research Service, USDA, in cooperation with the Department of Agronomy, Cornell University. The work was supported in part by the Meteorology Department, U. S. Army Electronics Research & Development Activity, Fort Huachuca, Arizona. Presented 4 April 1963 to the 5th Conference on Agricultural Meteorology in Lakeland, Florida. Dept. of Agronomy Series Paper No. 633.

2/ Agriculturist, Agricultural Research Service, USDA and Division of Meteorology, National Institute of Agricultural Sciences, Nishigahara, Tokyo, Japan; formerly Soil Scientist (Physics), USDA, now Graduate Assistant, Department of Agronomy, Cornell University, Ithaca, N. Y.

The methods of correlogram and spectral analysis are adopted for specifying the characteristics of turbulence within the plant-air layer. Results so obtained indicate that the similarity theory of turbulence can be applied to the plant-air layer where divergence in momentum flux occurs. A comparison of the spectral curve between the surface air layer and plant-air layer indicates that the ragged nature of the curve within the plant-air layer may tentatively be attributed to the waving and fluttering of plant leaves.

1. INTRODUCTION

The micrometeorological study of the photosynthesis of organic matter by land plants includes the study of both light absorption and energy and matter transfer (especially CO_2 and H_2O) between plant leaves and the surrounding air. The methods of measurement and analysis of these processes of transfer have formerly been restricted to the surface air layer above the plants. In that surface layer the complications of sources and sinks do not exist, and an assumption of vertical fluxes constant with height can often be made. However, the extension of surface layer theory to the plant air layer is complicated by more than the necessity of allowing for sources and sinks. The kinematics of the air flow are also different. Therefore, the generalizations about fluctuation velocities, turbulent energy, and turbulent transfer which were learned in the study of the surface layer may not be valid for the plant-air layer.

It is desirable to retain for the study of the plant-air layer as many as possible of the concepts and definitions of the physical quantities which have contributed to the remarkable development of the micrometeorology of the surface air layer. Among these, mixing length holds a high place. A few papers with this approach have been published, (e.g., Poppendieck, 1949; Tan and Ling, 1961; Uchijima, 1962b; Stoller and Lemon, 1963; Wright and Lemon, 1962). In his paper concerning the vertical profiles of wind speed and temperature in orange groves and brushland, Poppendieck proposed an equation for the dependence of mixing length on height above the ground. In this equation, he used a coefficient of proportionality which exceeds von Karman's constant ($\kappa = 0.4$). This implies that the mixing length is larger than

for a surface air layer without vegetation. In a theoretical study of the wind profile in a plant-air layer, Tan and Ling assumed a linear increase in exchange coefficient with height. From the assumption that physical quantities must be continuous at the top of the vegetation, and the hypothesis that the mixing length increases linearly with height in the vegetation, Uchijima introduced the plant layer constant, γ .

A few papers have attempted the experimental determination of the mixing length in plant-air layers. Baumgartner (1956) has evaluated the mixing length in a young fir forest, assuming $\ell = \kappa (z - d + z_o)$ in the height interval from the displacement height d up to the tree tops (at z = H), where κ , which has a value of 0.4 is von Karman's constant, and z_o is the roughness parameter. Stoller and Lemon (1963) made the assumption that turbulence is approximately isotropic in the plant-air layer, and used the Eulerian space scale of turbulence as a mixing length. However, Wright and Lemon (1962) in a further study have shown that this assumption was not valid.

None of these theoretical or partly experimental studies is conclusive. The understanding of the kinematics of air flow within the plant-air layer in relation to photosynthesis has yet to be won. This situation seems to be due to a lack of sufficiently good data.

Comprehensive measurements of air flow in a cornfield were made during the summer of 1962 in a cooperative USDA-Cornell University field study (Ithaca, New York) in much the same way they were made in 1961 by Wright and Lemon (1962). The data have been processed to provide the characteristics of air flow within the plant-air layer. The primary purpose of this paper is to present the available experimental results which are necessary to arrive at a reasonable understanding of the motion and structure of the air-flow within crop canopies of a cornfield. Presented also are some of the preliminary interpretations of the results.

2. SITE AND EXPERIMENTAL PROCEDURES

On three clear, sunny days, August 1-3, 1962, the horizontal wind speed,

$$V = \left\{ (\overline{u} + u')^2 + v'^2 \right\}^{1/2},$$

was measured in and above the vegetation of a 10-acre cornfield at Ellis Hollow, Ithaca, New York. The corn was 140 cm. tall, with a leaf area index of 3.8. The corn was densely planted in north-south rows 73 cm. apart, at a density of 29,000 plants per acre.

Simultaneous, overlapping vertical profiles were obtained with small cup anemometers (Thornthwaite Associates) and heated-thermocouple anemometers (Hastings-Raydist Co.)[3/]. The cup anemometers were mounted on a triangular tower at heights of 150, 170, 210, 290, 370, and 450 cm. above the ground. Cup rotation produced electrical signals, which were counted on pulse registers. The Hastings were also installed on the triangular tower, at heights of 50, 90, 110, 130, and 370 cm. above the ground. Thus, all of the cup anemometers were above the crop, while all of the thermocouple anemometers, with the exception of one, were within the plant-air layer. The electrical outputs from the Hastings were amplified and fed to individual, single-point recording milliammeters (Esterline Angus Electric Co.), giving a continuous record on

---

3/ For convenience the Hastings heated-thermocouple anemometers will be referred to simply as "Hastings" throughout this report. The anemometer probe of the Hastings consists of a series of thermocouples through which a small AC heating current is passed. Alternate junctions are cooled by mounting posts having higher thermal conductivity. The temperature difference between alternate junctions induces the thermoelectric potential which constitutes the signal. Air flow past the thermocouples decreases the temperature difference between alternate posts, thus also decreasing the thermoelectric current. The array of thermocouples is 2 cm. in diameter. The time constant of the individual thermocouples is of the order of 0.1 sec.

11.5 cm. chart paper. The response time of the amplifier and recorder limited the range of recording of rapid velocity fluctuations[4].

Ten-minute measurements of wind speed were taken at approximately hourly intervals during the period from 0900 to 1800 (EST) on each of the three days. Two banks of counters were used for the cup anemometers, and counts were recorded at intervals of 30 or 60 seconds. (This was done to obtain some measure of turbulent velocity in the surface layer above the plant-air layer.) For the plant-air layer, a test showed that reading the Hastings chart records at 5-second intervals was just as good as reading them at 1-second intervals for determining mean velocity and turbulent velocity. Therefore, the 5-second data interval was adopted.

In addition to the analyses of the 10-minute records, some special studies were made of selected 4-minute periods that showed no trends in mean speed. For studies of the micro-structure of turbulence, the 1-second data interval ($_{*}t$) was used.

---

[4] The DC, chopper stabilized amplifiers had a frequency response time of 2 cycles per second. The recorders had a full span response time of about 1 sec.

3. VERTICAL PROFILES OF METEOROLOGICAL ELEMENTS IN THE PLANT-AIR LAYER

A. Wind Speed

From all of the observations taken throughout the three test days, seventeen runs were chosen for a study of the wind system in and above the corn plant-air layer (see Table 1). The results shown in Table 1 include several properties of the wind profile. Among these are mean wind velocity, turbulent wind velocity, intensity of turbulence, reference wind velocity (U_H), roughness length in the plant-air layer (z_o'), and parameters A_o and B_o.

The mean wind speeds obtained by using the cup and Hastings anemometers are entirely comparable, since they are simultaneous and have the same sampling time (t_*). The turbulent velocities, however, are different for the two instruments. For the Hastings,

$$\sqrt{\overline{u'^2}} = \left[\overline{(u(t)-\bar{u})^2}\right]^{1/2}, \qquad z \leq H$$

while for the cup anemometers,

$$\sqrt{\overline{u'^2}} = \left[\overline{(\bar{u}_{60}-\bar{u})^2}\right]^{1/2} \qquad z \geq H$$

Here, u(t) is the instantaneous speed, $\bar{u}$ is the mean speed for the 10-minute period, and $\bar{u}_{60}$ is the mean speed for sampling time t_* = 60 seconds. The turbulent velocity determined by the second equation is necessarily less than that determined by the first, since it excludes contributions of eddies with a period less than 60 seconds. See discussions by Inoue (1947) and Ogura (1953).

To eliminate the peculiarities of the individual 10-minute profiles, a mean generalized profile was computed. It is the mean of 17 profiles normalized by

$$\Phi(z) = \frac{\bar{u}_z}{u_H}, \qquad (3.1)$$

TABLE 1.- Some quantities related to wind profile in corn plant-air layer.

Run no	Date	Item: z cm.	50 *	90 *	110 *	130 *	150 **	170 **	210 **	290 **	370 **	450 **	$\bar{U}_H$ cm/sec.	z_o' cm.	A_o cm/sec	B_o cm/sec
1	Aug.1	$\bar{u}$	14.5	14.8	25.8	55.1	93.9	104.0	120.5	139.2	146.3	157.1				
	1557	$(\overline{u'^2})^{1/2}$	5.7	5.9	19.2	48.2							84	3.0	21.8	58.0
	1607	$(\overline{u'^2})^{1/2}/\bar{u}$	39.4	39.8	74.4	87.5										
2	Aug.1	$\bar{u}$	10.5	10.7	16.9	35.0	70.7	78.7	96.5	108.5	121.1	128.0				
	1705	$(\overline{u'^2})^{1/2}$	2.6	4.1	8.1	24.9	18.4	20.3	20.9	27.2	26.6	29.8	57	2.1	13.6	40.0
	1715	$(\overline{u'^2})^{1/2}/\bar{u}$	24.3	38.3	47.9	71.1	26.0	25.8	21.7	25.1	22.0	23.3				
3	Aug. 1	$\bar{u}$	9.4	8.6	11.4	21.6	42.6	47.5	53.1	60.7	63.6	65.6				
	1823	$(\overline{u'^2})^{1/2}$	1.1	1.6	2.0	6.2	8.2	10.7	12.6	15.7	15.8	17.7	36	1.0	7.3	24.0
	1833	$(\overline{u'^2})^{1/2}/\bar{u}$	11.7	18.6	17.5	28.7	19.2	22.5	23.7	25.9	24.8	27.0				
4	Aug.	$\bar{u}$	14.3	17.1	25.2	47.9	90.9	103.3	120.6	147.4	168.7	195.6				
	1930	$(\overline{u'^2})^{1/2}$	7.0	7.9	17.8	40.9	29.1	28.2	35.5	44.5	45.2	50.8	77	3.5	20.8	51.0
	1940	$(\overline{u'^2})^{1/2}/\bar{u}$	48.5	46.2	70.6	85.4	32.0	27.3	29.4	30.2	26.8	26.0				
5	Aug. 1	$\bar{u}$	15.1	17.8	27.2	51.3	104.8	118.8	140.8	169.1	189.2	215.2				
	2020	$(\overline{u'^2})^{1/2}$	6.7	8.9	19.4	40.5	31.6	35.4	40.6	44.4	51.9	62.5	92	2.1	21.9	54.0
	2030	$(\overline{u'^2})^{1/2}/\bar{u}$	44.1	50.0	71.3	78.9	30.2	29.8	28.8	26.3	27.4	29.0				
6	Aug. 2	$\bar{u}$	15.6	16.0	24.1	61.3	92.6	104.8	116.7	132.3	145.5	172.4				
	0940	$(\overline{u'^2})^{1/2}$					47.7	50.6	64.3	77.5	87.2	91.2	78	0.9	15.4	61.0
	0950	$(\overline{u'^2})^{1/2}/\bar{u}$					51.5	48.3	55.1	58.6	59.9	52.9				
7	Aug. 2	$\bar{u}$	22.9	28.2	37.0	82.2	180.7	213.2	255.7	303.7	353.3	-				
	1011	$(\overline{u'^2})^{1/2}$											150	0.9	29.9	107.0
	1021	$(\overline{u'^2})^{1/2}/\bar{u}$														
8	Aug. 2	$\bar{u}$	22.0	31.0	-	77.6	146.7	165.7	190.1	230.4	255.2	273.2				
	1040	$(\overline{u'^2})^{1/2}$	11.2	31.6	-	68.1	70.2	88.0	98.4	121.2	134.3	143.5	134	3.8	37.1	88.0
	1050	$(\overline{u'^2})^{1/2}/\bar{u}$	50.8	101.9	-	87.7	47.8	53.1	51.8	52.6	52.6	52.5				
9	Aug. 2	$\bar{u}$	19.9	25.8	34.0	117.1	125.6	146.9	167.9	198.5	221.6	243.6				
	1223	$(\overline{u'^2})^{1/2}$	8.3	17.1	26.5	79.5	35.6	42.4	51.5	65.4	73.8	93.1	116	3.8	32.1	80.0
	1233	$(\overline{u'^2})^{1/2}/\bar{u}$	41.5	66.3	77.9	67.9	28.3	28.9	30.7	32.9	33.3	38.2				
10	Aug. 2	$\bar{u}$	22.2	31.2	41.2	-	181.1	208.9	247.3	293.3	324.4	355.2				
	1323	$(\overline{u'^2})^{1/2}$					25.9	33.6	43.6	53.2	58.8	64.7	169	2.9	43.8	120.0
	1333	$(\overline{u'^2})^{1/2}/\bar{u}$					14.3	16.1	17.6	18.1	18.1	18.2				
11	Aug. 2	$\bar{u}$	24.3	30.8	44.4	108.5	170.4	196.3	232.9	268.8	296.6	318.8				
	1407	$(\overline{u'^2})^{1/2}$	15.6	20.9	33.6	67.5	54.9	58.8	67.9	80.4	91.6	98.4	152	2.8	38.9	106.0
	1417	$(\overline{u'^2})^{1/2}/\bar{u}$	63.3	67.8	75.7	62.2	32.2	29.9	29.2	29.9	30.9	30.9				
12	Aug. 2	$\bar{u}$	17.3	20.6	33.0	88.2	157.5	166.4	-	230.2	255.1	278.5				
	1516	$(\overline{u'^2})^{1/2}$	6.6	12.4	24.2	58.6	35.1	39.1	-	57.2	63.0	73.6	135	3.3	36.0	100.0
	1526	$(\overline{u'^2})^{1/2}/\bar{u}$	37.5	60.2	73.3	66.4	22.3	23.5	-	24.8	24.7	26.4				

(cont.) (cont.)

Table 1, cont.

Run no	Date	Item \ Z cm.	50 *	90 *	110 *	130 *	150 **	170 **	210 **	290 **	370 **	450 **	$\bar{U}_N$ cm/sec.	z_o' cm.	A_o cm/sec.	B_o cm/sec.
	Aug. 2	$\bar{u}$	19.3	21.2	30.7	86.6	140.0	157.5	184.4	211.9	231.1	249.2				
13	1630	$(\overline{u'^2})^{1/2}$	10.6	10.2	22.9	56.5	22.8	27.3	29.8	38.9	31.8	49.3	125	2.4	30.7	84.0
	1640	$(\overline{u'^2})^{1/2}/\bar{u}$	54.8	48.1	74.6	65.2	16.3	17.3	16.2	18.4	13.8	19.8				
	Aug. 2	$\bar{u}$	13.9	16.0	22.2	55.0	105.3	117.5	138.3	164.4	179.1	188.6				
14	1722	$(\overline{u'^2})^{1/2}$	5.2	10.0	17.0	39.7	31.4	36.5	47.2	58.4	63.2	67.9	90	2.3	21.8	70.0
	1732	$(\overline{u'^2})^{1/2}/\bar{u}$	37.5	62.3	76.6	72.2	29.8	31.1	34.1	35.5	35.3	36.0				
	Aug. 3	$\bar{u}$	17.8	18.9	22.7	50.2	111.7	132.8	169.0	197.7	207.7	219.0				
15	0910	$(\overline{u'^2})^{1/2}$	7.1	9.1	11.7	34.2	17.9	25.2	27.7	29.0	29.7	29.4	95	2.6	23.8	65.0
	0920	$(\overline{u'^2})^{1/2}/\bar{u}$	39.4	48.3	51.5	64.1	16.0	18.9	16.4	14.7	14.3	13.4				
	Aug. 3	$\bar{u}$	17.5	20.4	23.4	61.2	113.3	128.8	154.2	186.2	205.9	-				
16	1020	$(\overline{u'^2})^{1/2}$					11.4	14.1	14.1	33.1	42.1	-	95	1.2	19.1	67.0
	1030	$(\overline{u'^2})^{1/2}/\bar{u}$					10.1	10.9	9.1	17.8	20.4	-				
	Aug. 3	$\bar{u}$	18.9	22.2	31.1	74.0	125.3	143.3	170.5	205.0	226.5	243.0				
17	1035	$(\overline{u'^2})^{1/2}$	8.0	12.6	32.4	53.9	46.7	52.2	66.2	91.9	103.9	108.6	110	2.7	27.8	75.0
	1045	$(\overline{u'^2})^{1/2}/\bar{u}$	42.1	54.7	104.1	72.8	37.3	36.4	38.8	44.8	45.9	44.7				

* and ** denote wind velocity from heated thermocouple and cup anemometers, respectively.

where $\bar{u}_z$ and $\bar{u}_H$ are 10-minute means at height z and the reference height z = 140 cm (crop height), respectively. The value of the wind velocity at crop height was determined by interpolating the wind velocity measured in and above the corn plant-air layer. The mean value of $\bar{\Phi}(\xi)$ and its standard deviation are shown in Figure 1.

Figure 1 shows that the 17 normalized wind profiles were similar in general, with a coefficient of variance of about 6.5% both in the crop and above it. This seems to say that the reference wind speed $\bar{u}_H$ has only a secondary role in the governing profile laws. The generalized wind profile (Fig. 1) shows a marked decrease of wind speed in the upper part of the plant-air layer, from 1.0 at 140 cm. to only 0.3 at 110 cm. In the lower part of the plant-air layer, wind speed is nearly constant with height.

The fact that the wind speed is decreased in the upper part of the plant-air layer is in good agreement with results of other researchers (e.g., Fons, 1940; Waterhouse, 1956; Baumgartner, 1956; Rauner, 1958; Penman and Long, 1960; Fritschen and Shaw, 1961; Stoller and Lemon, 1963). Penman and Long have reported that the generalized wind profile in a wheat plant-air layer changes somewhat with the reference wind velocity. However, the generalized wind profile in the corn plant-air layer is considered to be independent of the reference wind velocity. Although the difference between the features of wind profiles of wheat and corn plant-air layers seems to result from the differences in the dynamic characteristics of the plant bodies, at the present stage of the study, it is difficult to deduce any physical explanations for this difference. On the other hand, the generalized wind profile differs appreciably from that theoretically proposed by Poppendieck (1949). As already mentioned, this difference seems to be due to a faulty assumption by Poppendieck concerning the mixing length in the plant-air layer.

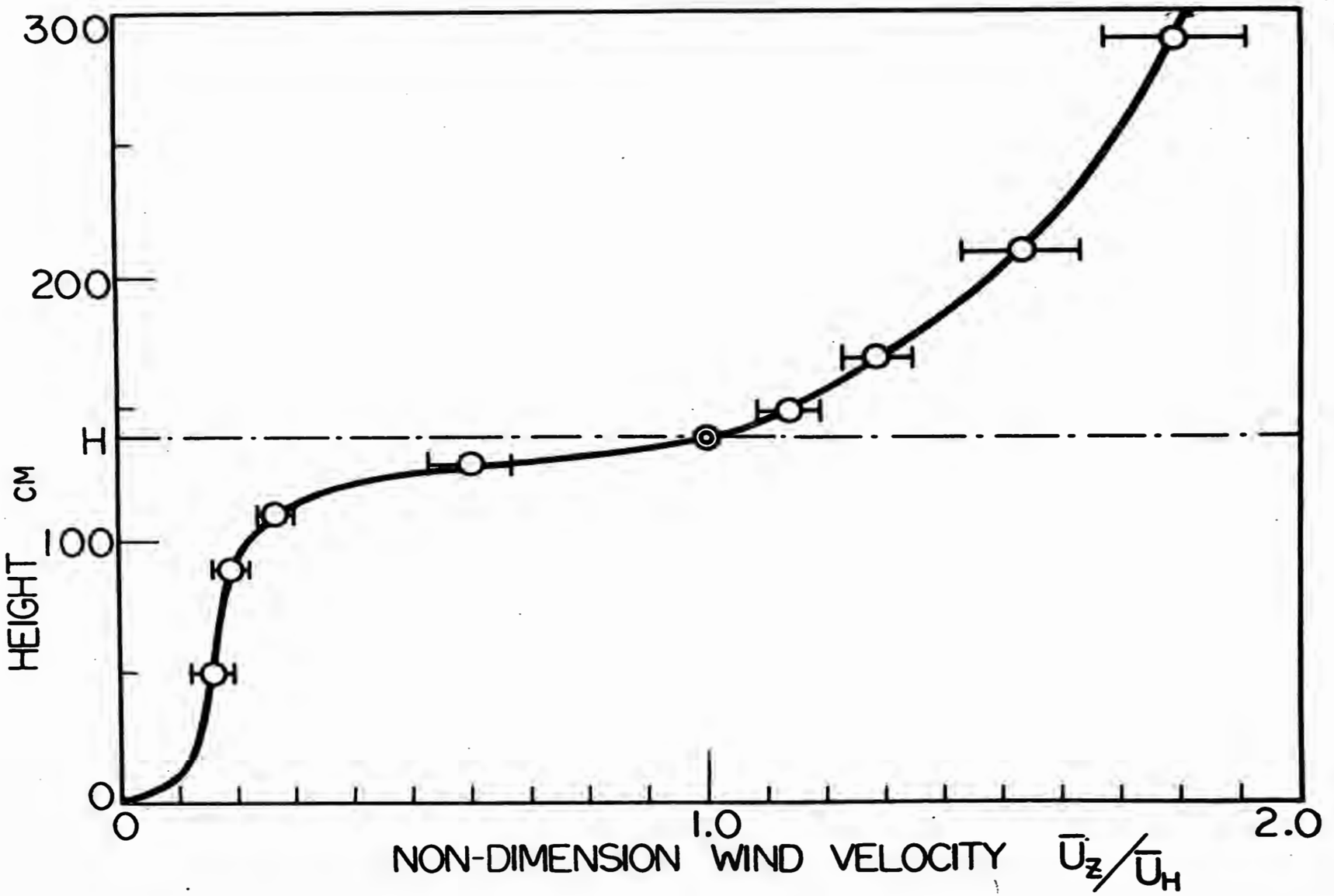

FIG. 1. GENERALIZED WIND PROFILE IN AND ABOVE PLANT-LAYER.

Under our experimental conditions, when the wind velocity at the reference height (H) was less than about 50 cm/sec., a constant-wind profile was frequently observed in the lower part of the plant-air layer. This may be due in part to heat convection from the heated-thermocouple anemometers. Fons (1940) has reported that the wind profiles in the forest and brush are affected by both reference wind speed and thermal stratification in the plant-air layer. However, our measurements do not show any considerable thermal effects, although thermal stratification ranged from super-adiabatic to inversion conditions. A simultaneous measurement of the temperature profile in the surface air layer over the cornfield was made using fine thermocouples.

The generalized wind profile shown in Figure 1 was approximated by an empirical equation as follows:

$$\overline{u}_z = \overline{u}_H + A_0 \ln \frac{z}{H} - B(z), \qquad z_0' \leq z \leq H \tag{3.2}$$

where $A_0 = f(\overline{u}_H)$ is a proportionality constant depending upon the reference wind velocity. The above empirical equation for the wind profile in the corn plant-air layer is considered to satisfy the following conditions:

$$\begin{aligned} &\overline{u}_z = \overline{u}_H && z \to H \\ &\overline{u}_z \propto \ln z && B(z) = 0 \\ &B(z) = f(\overline{u}_H, F(z)) \end{aligned} \tag{3.3}$$

where B(z) is an unknown function representing the influence of the plant community on wind velocity. The first condition shows continuity in the velocity profiles of the surface air and plant-air layers. The second indicates that the profile in the plant-air layer reduces to the logarithmic form for the limiting case of no plants. The third condition shows the departure from the logarithmic form.

In order to investigate the significance of this profile equation, the relative wind speed ($\bar{u}_z - \bar{u}_H$) was plotted against logarithmic height above the ground. The profiles, and the derived B(z), are shown in Figure 2. In Figure 2, extrapolation of the wind profile in the plant-air layer gives u = 0 at $z = z_o'$. This height will be called the roughness length for air flow in the layer. The straight line drawn between the two points (H,0) and $(z_o' , -\bar{u}_H)$ gives the logarithmic term in Eq. (3.2). The constant, A_o, can be determined from:

$$A_o = \frac{-\bar{u}_H}{\ln \frac{z_o'}{H}} = \frac{\bar{u}_H}{\ln \frac{H}{z_o'}} \quad . \tag{3.4}$$

The horizontal discrepancy between the $A_o \ln \frac{z}{H}$ - line and the $(\bar{u}_z - \bar{u}_H)$ - curve gives the function B(z), representing the effect of the vegetation. As $\bar{u}_H$ increases, B(z) increases without apparent change in shape. This implies that B(z) can be normalized to:

$$B'(z) = \frac{B(z)}{B_o} \quad ; \qquad z_o' \leq z \leq H \tag{3.5}$$

where B_o is the maximum value of B(z). It was suspected that the normalized B'(z) was related to F(z), which is the leaf area per unit volume of the plant-air layer (see Figure 2). They are seen to be similar, but not identical. Similar results were obtained for wheat and tall, mature corn, by re-analyzing wind data reported by Stoller and Lemon (1963). In this case, it was noted that the shape of B'(z) varied in a somewhat similar manner with that of the change in the profile of F(z).

The dependence of A_o and B_o on the reference wind velocity is illustrated in Figure 3. This figure shows that both constants are proportional to wind speed as follows:

$$\begin{aligned} A_o &= 0.25\ \bar{u}_H \ , \\ B_o &= 0.68\ \bar{u}_H \ . \end{aligned} \tag{3.6}$$

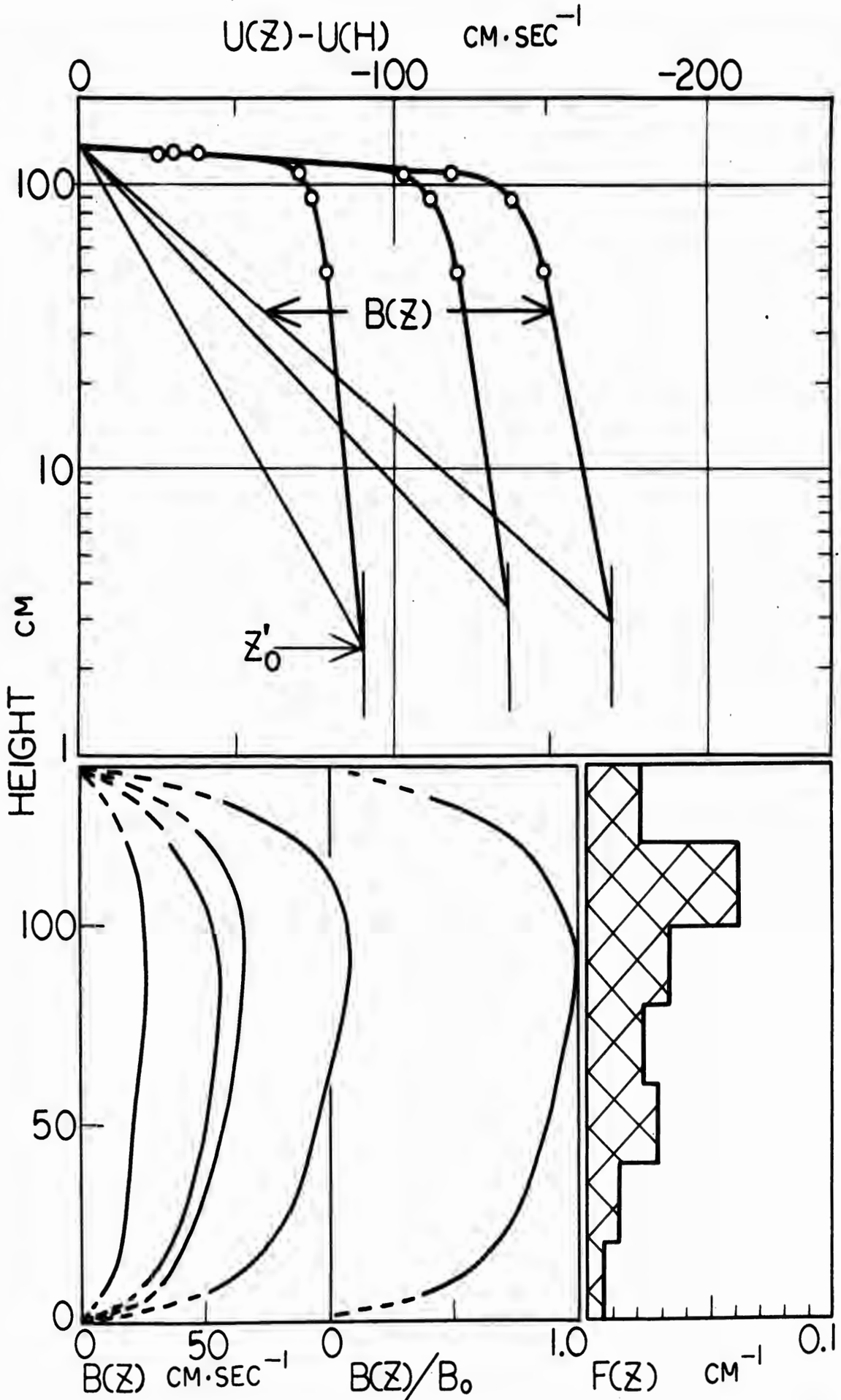

FIG. 2. VERTICAL PROFILES OF WIND AND RELATED QUANTITIES.

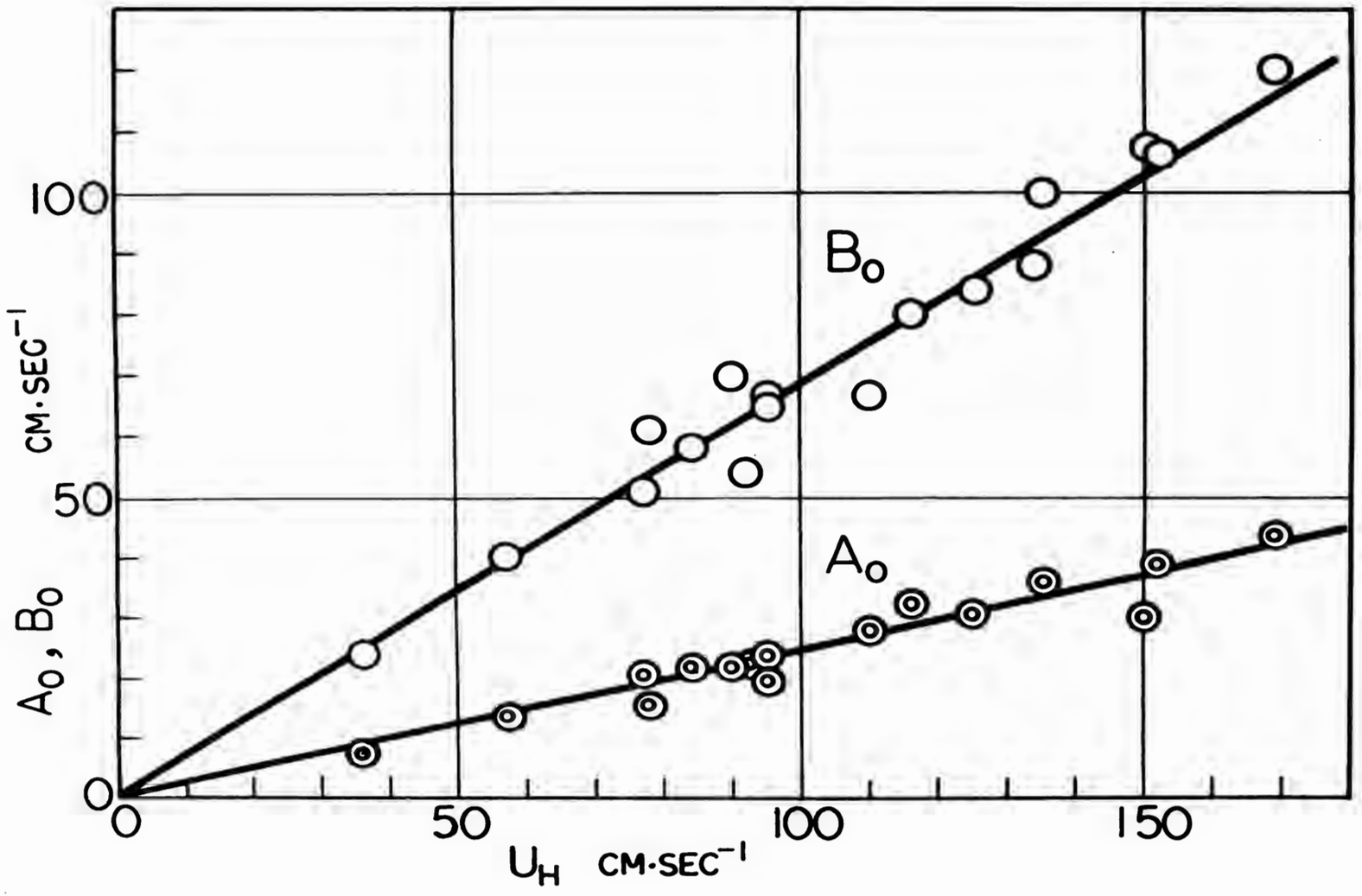

FIG. 3. DEPENDENCE OF PARAMETERS, A_o. B_o, ON WIND VELOCITY.

Substituting the above relations into Eq. (3.2) gives:

$$\bar{u}_z = \bar{u}_H + 0.25\,\bar{u}_H \ln\frac{z}{H} - 0.68\,\bar{u}_H B'(z)\;;\; z_0' \le z \le H \quad (3.7)$$

This is the empirical equation describing the wind profile in the plant-air layer of the corn crop, where the function B'(z) or B'($\frac{z}{H}$) characterizes the influence of the vegetation on air flow. Further study is needed to show whether this type of profile equation is suitable for plant-air layers having different crop structures.

B. Shearing Stress and Friction Velocity

It might be plausible to consider that even in the case of air-flow within plant-air layers, shearing stress (or friction velocity $v_* = \sqrt{\frac{\tau}{\rho}}$), as well as mixing length (to be discussed later), should be as useful in explaining the properties of air-flow in the plant-air layer as in the surface air-layer. Several studies have already estimated the vertical profile of shearing stress in the plant-air layer. Uchijima (1962 b) has reported that shearing stress decreases rapidly in the upper part of a paddy canopy. Monteith (1962) evaluated the shearing stress in a dense stand of beans, and suggested that under the foliage it has a value only 0.001 of its value above the crop.

In determining the shearing stress and friction velocity from measurements of wind speed and plant density in a plant-air layer, the following assumptions were made:

$$\begin{aligned} &\tau(z) = \tau_H - \rho\int_z^H C_z F(z)\,\overline{u_z^2}\,dz\,, \\ &\tau(0) \simeq 0\,, \\ &C_z \simeq \text{const.} = C\,, \end{aligned} \quad (3.8)$$

where $\tau(z)$ and τ_H are the shearing stress at a height z and at the top boundary of the plant-air layer, and C and F(z) denote the drag coefficient and leaf area per unit volume, respectively. Under dense foliage, it is safe to assume that shearing stress at the ground surface is negligibly small.

The drag coefficient in the vegetation is defined by:

$$C = \frac{2F_D}{\rho \overline{u_z^2}},$$

where F_D is the drag force per unit surface area of leaves. The vertical divergence of momentum flux may thus be expressed as:

$$\frac{d\tau}{dz} = 2F_D \cdot F(z) = \rho C F(z) \overline{u_z^2}. \tag{3.9}$$

The drag coefficient, C, is considered to be a function of "Reynolds' number" $Re = \frac{\bar{u} \cdot l}{\nu}$ (where $\bar{U}$ is the mean wind velocity, l the width of a leaf, and ν the kinematic viscosity of air). Considering the intensive absorption of momentum in the upper part of plant-air layers where relatively high wind velocity exists, that is where large Re-numbers ($2.5 \times 10^3 \sim 1 \times 10^4$) are observed, the drag coefficient for a corn plant-air layer can be assumed to be constant.

Using the above assumptions, the following relationship is obtained for the drag coefficient:

$$C = \frac{\tau_H}{\rho \int_0^H F(z) \overline{u_z^2}\, dz}. \tag{3.10}$$

The value of C (assumed to be constant) is obtained from the wind profile within the plant-air layer and the shearing stress at the upper boundary of the plant-air layer. $\tau(z)$ may be computed by Eq. (3.8), using data of F(z), $\bar{u}_z$, and τ_H. The results are presented in Table 2 and Figure 4.

As can be seen in Table 2, the drag coefficient ranges in value from 0.047 to 0.54, with a mean value of 0.17. A plot of C against $\bar{u}_H$ shows much scatter. The drag coefficient seems to decrease only slightly with wind speed.

The shearing stress and friction velocity are greatly diminished in the upper part of the plant-air layer. This agrees with results obtained in paddy

TABLE 2.- Vertical profiles of shearing stress, friction velocity, exchange coefficient and mixing length in the corn-air layer, (Aug. 1 - 3, 1962).

z	Item \ Run no	1	2	3	4	5	6 (cont.)
140	τ dyne/cm^2	0.699	0.521	0.039	0.390	0.655	0.293
	V_* cm/sec.	24.1	20.8	5.7	18.0	23.5	15.6
	K cm^2/sec.	530.2	457.6	125.4	396.0	517.0	343.2
	ℓ cm.	22.0	22.0	22.0	22.0	22.0	22.0
120	τ dyne/cm^2	0.293	0.228	0.019	0.181	0.291	0.142
	V_* cm/sec.	15.6	13.7	4.0	12.2	15.5	10.8
	K cm^2/sec	324.5	288.7	40.0	215.7	293.0	166.0
	ℓ cm.	20.8	21.1	10.0	17.8	18.9	15.4
100	τ dyne/cm^2	0.078	0.055	0.007	0.053	0.086	0.034
	V_* cm/sec.	8.1	6.8	2.4	6.6	8.4	5.3
	K cm^2/sec.	298.1	142.2	57.6	218.0	294.2	140.5
	ℓ cm.	37.3	20.9	24.0	33.0	35.0	26.5
80	τ dyne/cm^2	0.036	0.025	0.004	0.028	0.040	0.016
	V_* cm/sec.	5.5	4.5	1.8	4.8	5.7	3.6
	K cm^2/sec.	178.2	134.0	46.2	153.0	180.6	86.0
	ℓ cm.	32.4	29.9	25.7	31.9	31.7	23.9
60	τ dyne/cm^2	0.011	0.013	0.0026	0.013	0.021	0.008
	V_* cm/sec.	3.0	3.3	1.4	3.3	4.1	2.6
	K cm^2/sec.	56.3	99.0	27.8	72.6	93.3	45.3
	ℓ cm.	18.8	30.0	19.8	22.0	22.8	17.4
40	τ dyne/cm^2	0.005	0.003	0.0009	0.003	0.006	0.001
	V_* cm/sec.	2.0	1.5	0.8	1.5	2.2	0.9
	K cm^2/sec.	17.4	22.5	9.1	10.9	19.2	36.4
	ℓ cm.	8.7	15.0	11.4	7.3	8.7	40.4
20	τ dyne/cm^2	0.002	0.001	0.0005	0.001	0.002	0.0005
	V_* cm/sec.	1.2	0.9	0.6	0.9	1.3	0.6
	K cm^2/sec.	9.3	10.1	6.0	5.7	10.6	2.8
	ℓ cm.	7.8	11.2	10.0	6.3	8.2	4.7
$C = \frac{\tau_H}{\rho \int_0^H F(z) \overline{u}_z^2 dz}$		0.179	0.274	0.047	0.108	0.138	0.072

Table 2.- (cont.) Vertical profiles. .

z	Item \ Run no	7	8	9	10	11	12 (cont.)
140	τ dyne/cm^2	2.834	0.821	0.599	2.055	1.967	1.249
	V_* cm/sec.	48.5	26.1	22.3	41.3	40.4	32.2
	K cm^2/sec.	1067.0	574.2	490.6	908.6	888.8	708.4
	ℓ cm.	22.0	22.0	22.0	22.0	22.0	22.0
120	τ dyne/cm^2	1.157	0.449	0.278	0.939	0.963	0.471
	V_* cm/sec.	30.9	19.3	15.2	27.9	28.3	19.8
	K cm^2/sec.	712.5	313.0	222.1	515.4	459.7	323.9
	ℓ cm.	23.1	16.2	14.6	18.5	16.2	16.4
100	τ dyne/cm^2	0.500	0.102	0.094	0.192	0.220	0.118
	V_* cm/sec.	20.4	9.2	8.8	12.6	13.5	9.9
	K cm^2/sec.	1067.2	241.7	258.0	360.9	455.5	280.0
	ℓ cm.	52.3	26.3	29.3	28.6	33.7	28.3
80	τ dyne/cm^2	0.206	0.050	0.053	0.100	0.114	0.058
	V_* cm/sec.	13.1	6.5	6.6	9.1	9.7	6.9
	K cm^2/sec.	591.7	156.7	189.6	376.3	313.7	176.2
	ℓ cm.	45.2	24.1	28.7	41.3	32.3	25.5
60	τ dyne/cm^2	0.108	0.028	0.032	0.056	0.062	0.031
	V_* cm/sec.	9.4	4.8	5.1	6.8	7.1	5.1
	K cm^2/sec.	304.8	88.4	113.0	250.9	168.7	100.0
	ℓ cm.	32.4	18.4	22.2	38.0	23.7	19.6
40	τ dyne/cm^2	0.022	0.010	0.014	0.019	0.018	0.007
	V_* cm/sec.	4.3	2.9	3.4	3.9	3.8	2.4
	K cm^2/sec.	45.1	22.7	36.3	32.3	49.6	15.7
	ℓ cm.	10.5	7.8	10.7	8.2	13.1	6.5
20	τ dyne/cm^2	0.001	0.005	0.010	0.010	0.005	0.002
	V_* cm/sec.	0.9	2.0	2.9	2.8	2.0	1.3
	K cm^2/sec.	2.9	16.7	40.0	26.0	14.3	7.1
	ℓ cm.	3.2	8.3	13.8	9.3	7.2	4.2
	$C = \dfrac{\tau_H}{\rho \int_0^H F(z)\, \bar{u}_z^2\, dz}$	0.275	0.055	0.071	0.113	0.122	0.133

Table 2.- (cont.) Vertical profiles . .

z	Item \ Run no	13	14	15	16	17
140	τ dyne/cm^2	1.042	1.056	2.429	0.992	1.596
	V_* cm/sec.	29.4	29.6	44.9	28.7	36.4
	K cm^2/sec.	646.8	651.2	987.8	631.4	800.8
	ℓ cm.	22.0	22.0	22.0	22.0	22.0
120	τ dyne/cm^2	0.451	0.391	0.964	0.473	0.699
	V_* cm/sec.	19.3	18.3	28.3	19.8	24.1
	K cm^2/sec.	332.6	334.9	942.2	461.2	592.6
	ℓ cm.	17.2	18.3	33.3	23.3	24.6
100	τ dyne/cm^2	0.154	0.118	0.352	0.155	0.230
	V_* cm/sec.	11.3	9.9	17.1	11.3	13.8
	K cm^2/sec.	386.9	408.3	1169.6	510.8	665.7
	ℓ cm.	34.2	41.2	68.3	45.2	48.2
80	τ dyne/cm^2	0.076	0.060	0.173	0.083	0.114
	V_* cm/sec.	7.9	7.0	11.9	8.3	9.7
	K cm^2/sec.	249.6	272.2	745.2	362.6	427.7
	ℓ cm.	31.6	38.8	62.6	43.7	44.1
60	τ dyne/cm^2	0.040	0.031	0.087	0.047	0.058
	V_* cm/sec.	5.7	5.1	8.5	6.2	6.9
	K cm^2/sec.	135.4	152.9	401.6	213.3	226.6
	ℓ cm.	23.8	29.9	47.2	34.4	32.8
40	τ dyne/cm^2	0.009	0.007	0.017	0.014	0.010
	V_* cm/sec.	2.7	2.4	3.7	3.4	2.9
	K cm^2/sec.	20.9	36.0	52.7	44.6	28.0
	ℓ cm.	7.7	15.0	14.2	13.1	9.7
20	τ dyne/cm^2	0.002	0.001	0.001	0.005	0.006
	V_* cm/sec.	1.3	0.9	0.9	2.0	2.2
	K cm^2/sec.	7.7	5.4	4.8	23.5	25.4
	ℓ cm.	4.5	6.0	5.3	11.8	11.5
$C = \frac{\tau_H}{\rho \int_0^H F(z)\, \overline{U}_z^{\,2}\, dz}$		0.120	0.259	0.542	0.176	0.233

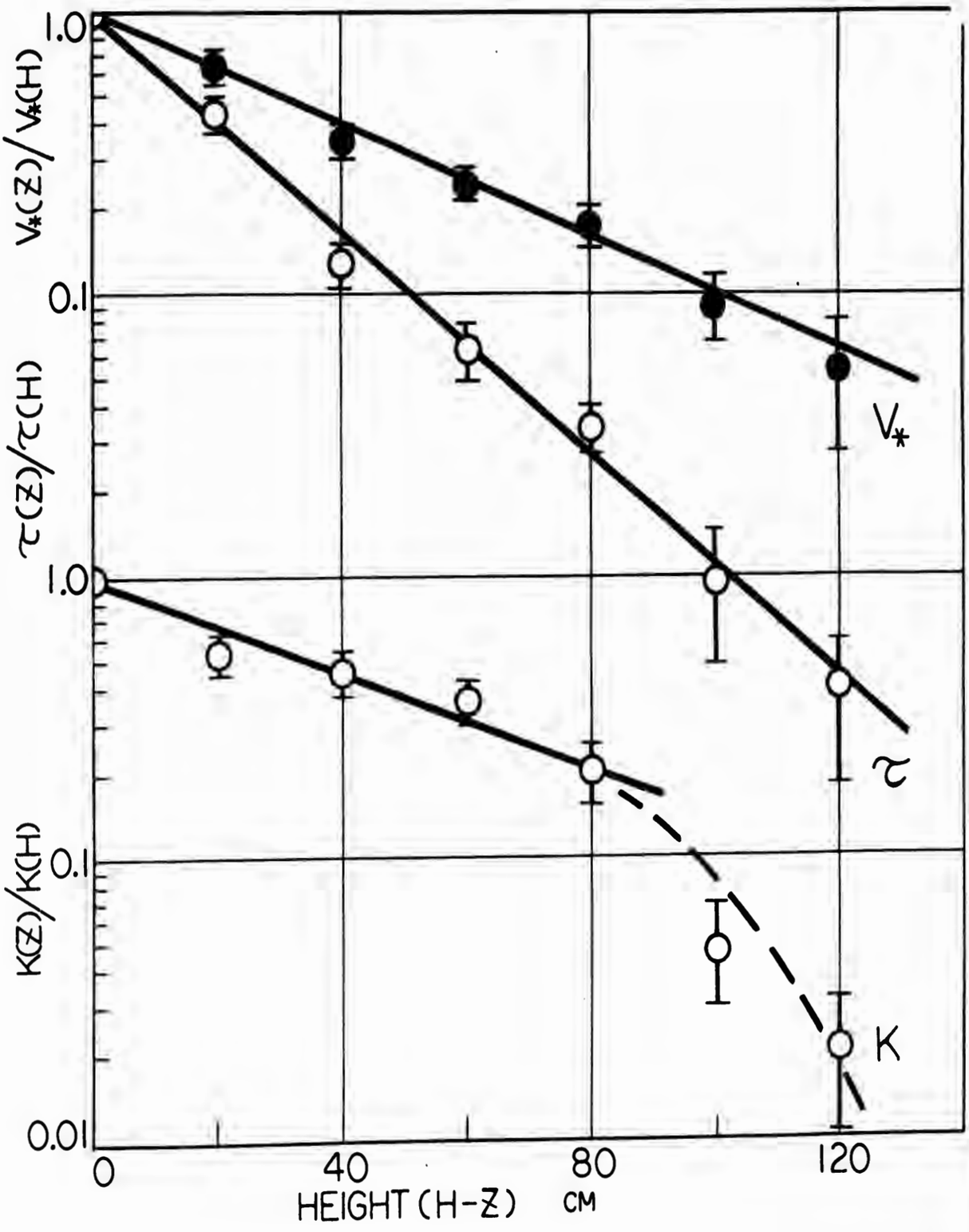

FIG. 4. VERTICAL PROFILES OF FRICTION VELOCITY, SHEARING STRESS, EXCHANGE COEFFICIENT.

fields (Uchijima 1962 b). The mean generalized profiles and the standard deviations for both $\frac{\tau(z)}{\tau_H}$ and $\frac{V_*(z)}{V_{*H}}$, based on 17 runs, are shown in Figure 4.

Figure 4 shows that the vertical profiles of these quantities within the plant-air layer can be approximated by an exponential law. Since τ is proportional to V_*^2, the constant contained in its exponential term is twice as large. The generalized relations are approximated by:

$$\tau(z) = \tau_H e^{-5.6\left(1-\frac{z}{H}\right)}, \qquad z_0' \leq z \leq H \qquad (3.11)$$

$$V_*(z) = V_{*H} e^{-2.8\left(1-\frac{z}{H}\right)}.$$

These relations imply that the momentum absorption term, on which the exchange coefficient in the plant-air layer depends, can be expressed as:

$$\left[1 - \frac{\rho \int_z^H C F(z) \overline{u_z^2}\, dz}{\tau_H}\right] \simeq e^{-\text{const}\left(1-\frac{z}{H}\right)}$$

Both the decrease of momentum flux and radiant energy flux approximate exponential laws.

C. Exchange Coefficient and Diffusion Resistance

In general, the exchange coefficient for shear flow is given by the mixing length theory as:

$$K = l \cdot V_*, \qquad (3.12)$$

where l is the mixing length (see below concerning the mixing length in the plant-air layer). From the values of shearing stress and wind speed in the plant-air layer, the exchange coefficient was calculated by:

$$K(z) = \frac{\tau(z)}{\rho\left(\frac{d\bar{u}}{dz}\right)_z} = \frac{\tau_H - \rho C \int_z^H F(z) \overline{u_z^2}\, dz}{\rho\left(\frac{d\bar{u}}{dz}\right)_z}. \qquad (3.13)$$

In calculating the exchange coefficient with the above equation, the value of the vertical gradient of wind speed was obtained by graphically differentiating the wind profiles of the plant-air layer.

The results are presented in Table 2 and Figure 4. The exchange coefficient decreased very rapidly with depth (H-z) into the plant-air layer. The magnitudes at the zero plane displacement height (d = 85 cm.) are 1/4 to 1/2 of those at the upper boundary of the plant-air layer. The height dependence of the exchange coefficient, except near the ground, can be approximated by the exponential equation:

$$K(z) = K_H e^{-2.8\left(1-\frac{z}{H}\right)} \qquad 60 \leq z \leq H \qquad (3.14)$$

Below z = 60 cm., K(z) decreases more rapidly than predicted by Eq. (3.14). A similar height dependence of the exchange coefficient has already been reported for a paddy field (Uchijima, 1962 a) and a wheat field (Saito, 1962). The value of the constant (2.8) in Eq. (3.14) is somewhat smaller than that (3.1) for a paddy field. As can be seen from a comparison of Eq. (3.14) with Eqs. (3.11) and (3.12), Eq. (3.14) seems to indicate that the vertical profile of the exchange coefficient in the upper part of the plant-air layer depends mainly upon the friction velocity, V_*. Also, the change of mixing length in this layer has no appreciable influence on the vertical profile of the exchange coefficient. On the other hand, in the plant layer below z = 60 cm., the decrease in the magnitude of the exchange coefficient is steeper than that from Eq. (3.14), implying that the variation of the mixing length should have an appreciable effect on the exchange coefficient.

Recently, "diffusive resistance" has come into use in considering plant-to-atmosphere transfer, where different transfer mechanisms (such as turbulent and molecular diffusion) are involved. Diffusive resistance of vertical transfer is related to the other well-known transfer coefficients by:

$$r_{z_1 \to z_2} = \frac{1}{D_{z_1 \to z_2}} = \frac{c_p \rho}{h_{z_1 \to z_2}} = \int_{z_1}^{z_2} \frac{dz}{K(z)} , \qquad (3.15)$$

where, $r_{z_1 \to z_2}$ is the diffusive resistance (sec/cm.),

$D_{z_1 \to z_2}$ is the integral exchange coefficient (cm/sec.),

$h_{z_1 \to z_2}$ is the sensible heat transfer coefficient (ly/sec.°C),

all defined for the height interval from z_1 to z_2.

The integral exchange coefficient, D, has been used mainly by Russian researchers (e.g., Budyko, 1956; Broido, 1957; Rauner, 1961; Medvedeva et al., 1962) for studying the heat balance. The heat transfer coefficient, h, has usually been utilized by Japanese researchers (e.g., Uchijima, 1959, 1961, 1962; Iwakiri, 1962; Kotoda et al., 1962) in the study of the heat balance of a paddy field.

By making use of Eq.(3.15), the diffusive resistance can be easily determined from other coefficients. It appears also from the above equation that the diffusive resistance of the air layer from z_1 to z_2 is affected most by the smallest value of the exchange coefficient in this layer.

In determining the diffusive resistance in the plant-air layer by Eq.(3.15) and the exchange coefficient, the following relations were used for the vertical profile of the exchange coefficient:

$$K(z) = K_H e^{-2.8\left(1 - \frac{z}{H}\right)}, \qquad 60 \leq z \leq H$$

$$K(z) = \frac{K_{60}}{60} \cdot z . \qquad 0 \leq z \leq 60$$

The results are presented as a function of wind velocity ($\bar{u}_H$) and resistance path-length (H-z) in Figure 5. The resistance for the whole path-length (H) is shown with the curve from the following relation,

$$r_{H \to 0} = \frac{\alpha}{\bar{u}_H} \qquad (3.16)$$

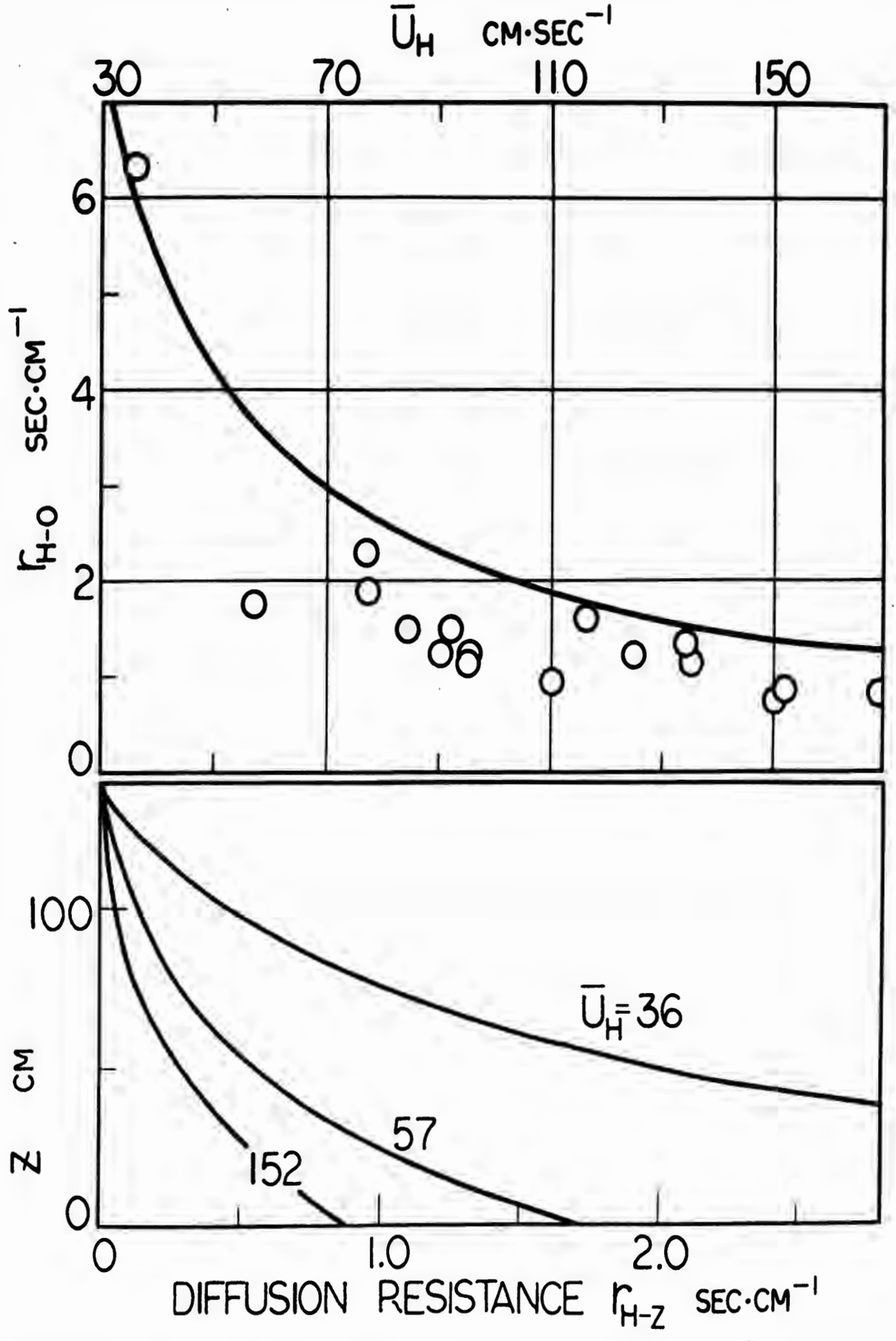

FIG. 5. DIFFUSION RESISTANCE AS FUNCTION OF WIND VELOCITY AND HEIGHT.

where,

$$\alpha = \frac{C \ln\left(\frac{H-d}{z_0}\right)}{\kappa^2 (H-d)} \quad , \quad C = 800.$$

As shown in figure 5, the diffusive resistance, $r_{H \to 0}$, decreases rapidly with increasing wind velocity, viz., from about 6.0 sec/cm. at 36 cm/sec. to 0.8 sec/cm. at 170 cm/sec. This shows a tendency toward good agreement with the results predicted by the hyperbolic function of $r_{H \to 0}$ as related to wind velocity (3.16). For wind velocities exceeding 100 cm/sec., the diffusive resistance is in the range 1.5 to 0.8 sec/cm. These values are close to those Monteith (1962) expected for the air layer between the soil surface and the zero plane displacement height in a wheat field. But the magnitude of the diffusive resistance for the corn plant-air layer was 1/4 to 1/2 less than that for a paddy field (Uchijima, Kotoda). This difference in the magnitude of the diffusive resistance seems to be an effect of the differences in crop structure between the two types of plant communities, namely the differences in the characteristics of the turbulence within the plant-air layers.

Figure 5 also shows the dependence of diffusive resistance $r_{H \to z}$ upon both wind velocity and the resistance path-length (H-z). The diffusive resistance $r_{H \to z}$ increases considerably with increasing resistance path-length, and the rate of increase depends highly upon the wind velocity at the top boundary of the plant-air layer. From the above description, it is apparent that the magnitude of the diffusive resistance for the whole resistance path-length is affected most by its larger values in the lower part of the plant-air layer.

D. Mixing Length

Although the mixing length, l , is an important variable governing air flow, the little that is known about it in plant-air layers comes from a few preliminary studies. In order to successfully apply the mixing length concept to the study of the air-flow within plant-air layers, an empirical and theoretical

relationship between it and a length characteristic of the plant-air layer is necessary.

According to Prandtl's mixing length theory, the mixing length in shear flow is given by:

$$l = \frac{V_*}{\left(\frac{d\bar{u}}{dz}\right)} \qquad (3.17)$$

It is assumed that the above equation applies also to the plant-air layer where momentum is absorbed. The values of the mixing length obtained from the above equation along with values of the friction velocity, V_*, and velocity gradient, $\left(\frac{d\bar{u}}{dz}\right)$ are given in Table 2. The mean mixing length profile of the plant-air layer and respective values of the standard deviation obtained from 17 runs are shown in Figure 6.

As seen in Figure 6, the mixing length, l, decreases from a value of 22 cm. at the upper boundary of the plant-air layer to one of 17 cm. at the 110-120 cm. layer where the highest density of F(z) is observed. At a height of about 100 cm., the mixing length shows an abrupt increase from a value of 12 cm. to one of about 30 cm., giving the appearance of discontinuity. In the region below 100 cm., the mixing length decreases gradually with decreasing height. In this region the mixing length may be expressed as:

$$l = 0.4\,(z + z_0') \qquad z_0' \leq z \leq 100\ cm.$$

The vertical profile of the mixing length described above seems to indicate that the influence of plant bodies on the mixing length itself is limited to the layer of highest leaf density F(z). It also appears that the well known relationship with von Karman's constant, $\kappa = 0.4$, can be applied to the plant-air layer with a considerably lower value of F(z). The experimental results obtained in the corn plant-air layer differ from those proposed by several other researchers (Poppendieck, 1949; Uchijima, 1962 b; Cionco, 1962; Stoller and Lemon, 1963). The results shown in Figure 6 are more complicated than those of the proposed hypotheses. Such a complicated vertical mixing

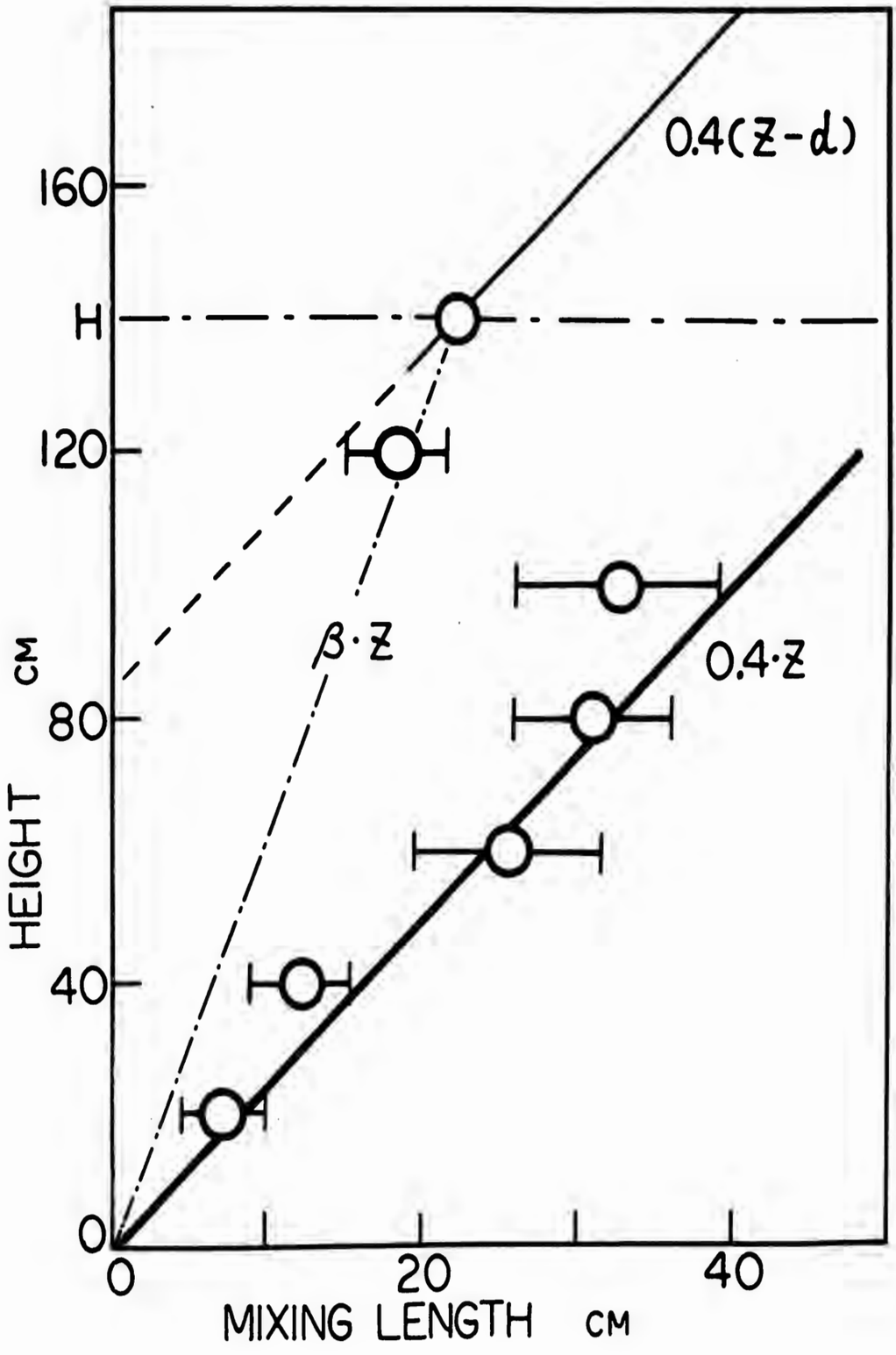

FIG. 6. VERTICAL PROFILE OF MIXING LENGTH IN PLANT-LAYER.

length profile in the corn plant-air layer seems to result from the inhomogeneous vertical arrangement of leaves. In order to determine a general law relating the mixing length to height within the plant-air layer, comprehensive observations of the air-flow patterns within the plant-air layers having various shapes, arrangement, and aerodynamic leaf properties of plant communities are needed. We hope that they will be carried out.

4. MICRO-STRUCTURE AND STATISTICAL PROPERTIES OF TURBULENCE IN THE PLANT-AIR LAYER

The micro-structure of turbulence in the plant-air layer accounts for many important phenomena in this layer. Serious interest in the measurement of the micro-structure of turbulence within this layer has arisen recently, but there are no experimental results comparable with those for a surface air layer. In agricultural meteorology, the importance of the micro-structure of turbulence in determining the exchange of energy and matter between the plant leaf and the air layer has been emphasized by several researchers: e.g., Waterhouse, (1955); Nakagawa, (1956); Inoue, (1962); Uchijima, (1962 a,b); Saito, (1962); Saito et al., (1962); and Stoller and Lemon, (1963).

Waterhouse measured wind velocity and turbulent velocity in meadows in order to investigate the qualitative characteristics of plant-air layers as insect environments. He reported that these quantities are greatly reduced in the top layer. From his analysis of wind velocity fluctuation data for a paddy field, Nakagawa has suggested that the horizontal scale of the largest eddies within the layer is nearly independent of height above the water surface. Inoue, Uchijima, and Saito have pointed out that an understanding of the micro-structure of turbulence in plant-air layers is important to an understanding of the exchange processes of the various physical quantities in the layers. Stoller and Lemon also have indicated the importance of studying the micro-structure of turbulence in the plant-air layer.

As described in Section (2), 20 records of the fine-fluctuation in wind velocity were analyzed, including one from a height of 370 cm., four from 130 cm., five from 110 cm., five from 90 cm., and five from 50 cm. Each record covered

a time interval of 4.0 minutes, during which no appreciable fluctuation in mean wind velocity was observed. Runs chosen for micro-structure of turbulence analysis included nearly the whole wind velocity range experienced in this study.

The mutually related methods of correlogram and spectral analysis were adopted for specifying the character of turbulence in the corn-plant-air layer. The results so obtained will be discussed and compared with those for the surface air layer using the similarity theory of turbulence.

A. Turbulent Velocity

Generally, the turbulent velocity, which is an important characteristic of the turbulent field, is given by:

$$\sqrt{\overline{u'^2}} = \left\{ \overline{(u(t) - \overline{u})^2} \right\}^{1/2} . \qquad (4.1)$$

Using the sampling period of 600-sec. and the observation interval of 5-sec., the values of the turbulent velocity and of the turbulent intensity, $\frac{\sqrt{\overline{u'^2}}}{\overline{u}}$ are calculated and are presented in Table 1. As shown in this table, the turbulent velocity at a height of 130 cm. is in the range of 6.2 to 79.5 cm/sec., with reference wind velocities of 36 to 170 cm/sec. As the plant-layer depth (H-z) increases, the turbulent velocity decreases greatly. At a height of 50 cm., the values range from only 1.1 to 15.6 cm/sec.

To obtain the general features of the vertical profile of the turbulent velocity in the plant-air layer, the turbulent velocity was generalized, using the following relation:

$$S = \frac{\left(\sqrt{\overline{u'^2}}\right)_z}{\left(\sqrt{\overline{u'^2}}\right)_{50}} , \qquad (4.2)$$

where $\left(\sqrt{\overline{u'^2}}\right)_{50}$ is the turbulent velocity at a height of 50 cm. The mean profile obtained from the data of the 13 runs is shown in Table 3.

TABLE 3.- Vertical profile of the generalized turbulent velocity ($S = \frac{(\sqrt{\overline{u'^2}})_z}{(\sqrt{\overline{u'^2}})_{50}}$) and the standard deviation.

Item \ Z cm.	130	110	90	50
s	6.83	2.82	1.56	1.00
σ_s	±1.73	±0.72	±0.47	-
c.v.	0.254	0.255	0.299	-

The values of the generalized turbulent velocity show that the decrease of turbulent velocity with depth in the plant-air layer should follow a unique law. Also, except for the lower part of the profile, the turbulent velocity is approximated by:

$$\left(\sqrt{\overline{u'^2}}\right)_z \simeq \left(\sqrt{\overline{u'^2}}\right)_H e^{-5.6\left(1-\frac{z}{H}\right)}, \qquad z_0 \le z \le H \qquad (4.3)$$

where $\left(\sqrt{\overline{u'^2}}\right)_H$ shows the value of the turbulent velocity at the plant height evaluated from profile extrapolation. By considering the micro-structure of turbulence, it is possible to semi-empirically determine the expression for the vertical profile of turbulent velocity in plant-air layers. In general, the structure function for a turbulent wind field is given by:

$$B_{dd} = 2\overline{u'^2}\left\{1 - Ru(l)\right\} = B_v{}^2 \cdot l^{2/3}, \qquad (4.4)$$

where,

B_{dd} is the structure function for a turbulent wind field,

$\overline{u'^2}$ is the mean value of turbulent velocity,

$Ru(l)$ is the Eulerian space correlation function in the mean wind direction,

l shows the separation distance in the mean wind direction,

B_v shows the structure parameter.

From the above relation, we have,

$$\sqrt{B_{dd}} = \sqrt{2}\sqrt{\overline{u'^2}}\left\{1 - R_u(l)\right\}^{1/2} = B_v \cdot l^{1/3} \qquad (4.4a)$$

Using the theoretical relation for the structure parameter and the empirical relation (3.11) for the vertical profile of the friction velocity in the plant-air layer, the structure parameter in the plant-air layer can be approximately expressed as follows:

$$B_v = \frac{C_1 \cdot V_{*H}}{[l(z)]^{1/3}} e^{-2.8\left(1 - \frac{z}{H}\right)}$$

By substituting this relation into Eq. (4.4a), and assuming that

$$R(l) \longrightarrow 0 \qquad \text{at } l \longrightarrow l^*$$

where l^* denotes the horizontal scale of the representative largest scale, it becomes

$$\sqrt{\overline{u'^2}} = \frac{C_1}{\sqrt{2}}\left[\frac{l^*}{l(z)}\right]^{1/3} V_{*H} e^{-2.8\left(1 - \frac{z}{H}\right)}, \qquad z_0 \le z \le H \qquad (4.5)$$

where,

C_1 is a universal constant, with a value of 1.11 (see Obukhov, 1958),

$l(z)$ denotes the mixing length at a height z,

V_{*H} is the friction velocity at the upper boundary of the plant-air layer.

This indicates that the turbulent velocity in the plant-air layer depends not only upon the friction velocity, but also upon the horizontal scale and the vertical scale of the representative largest eddy.

The decrease in turbulent velocity with increment of depth (H-z) agrees well with those for a meadow (Waterhouse, 1955) and paddy field (Nakagawa, 1956). The value of the turbulent velocity is represented in Figure 7 as a function of both reference wind velocity, $\overline{u}_H$, and height above ground surface.

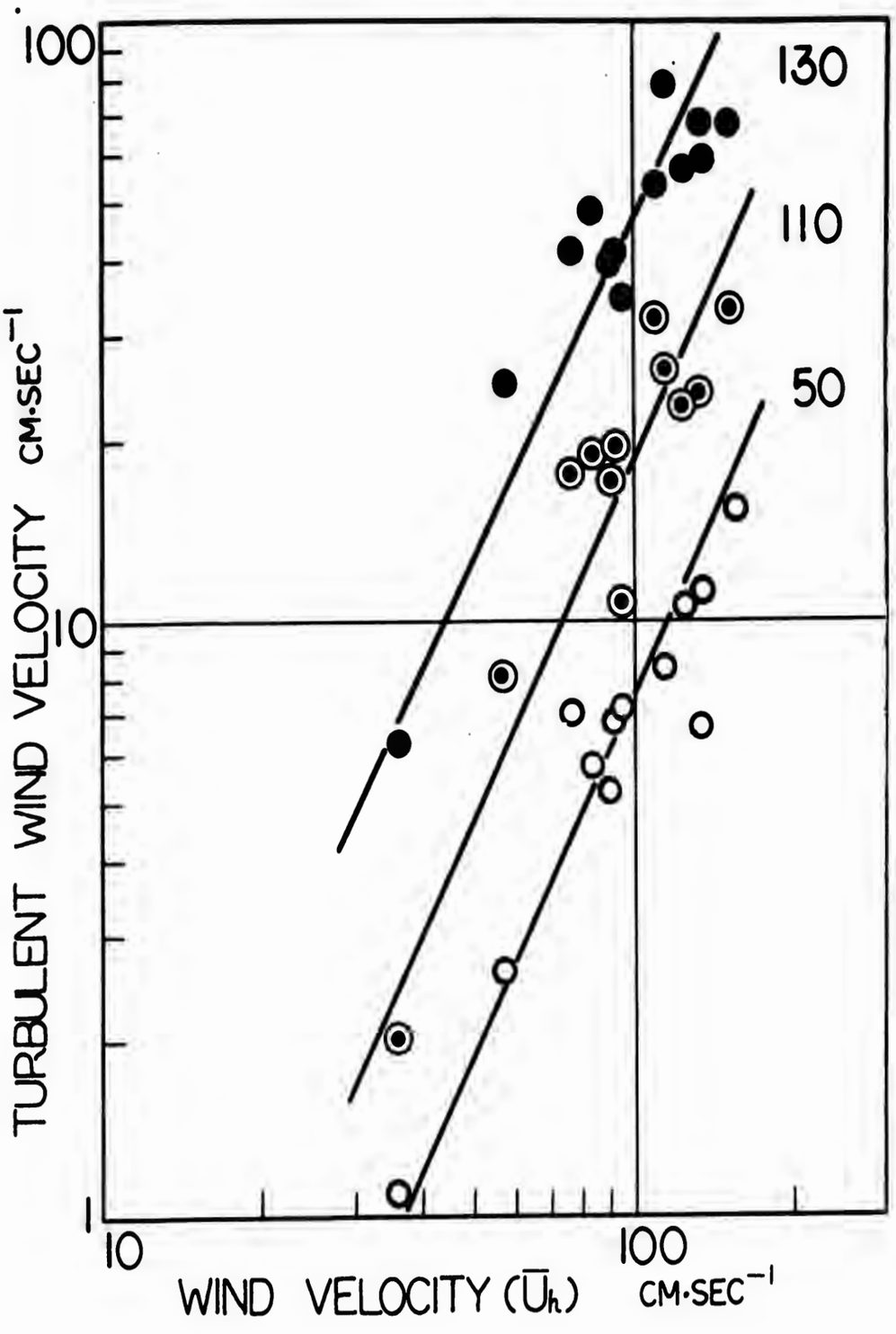

FIG. 7. DEPENDENCE OF TURBULENT VELOCITY ON WIND VELOCITY AND HEIGHT.

Although the points are scattered, the dependence of the turbulent velocity on the reference wind velocity, as is seen in Figure 7, can be approximated by,

$$\sqrt{\overline{u'^2}} \propto \bar{u}_H^2 . \qquad (4.6)$$

The existence of the above relation for heights within the plant-air layer provides evidence that the generalized vertical profile of turbulent velocity is independent of the reference wind velocity, $\bar{u}_H$.

Considering the data as a whole, turublent intensity, $\frac{\sqrt{\overline{u'^2}}}{\bar{u}}$, decreased gradually with depth (H-z). The value at a depth (H-z) of 90 cm. was 0.5 that at a depth (H-z) of 10 cm. On the other hand, Nakagawa's results for a paddy field indicate that the turbulent intensity is independent of height above the water surface. As can be seen in Table 1, it seems reasonable to consider the turublent intensity as a function decreasing with plant layer depth within this cornfield. The turbulent intensity is larger than that usually observed in a surface air layer. At 130 cm. height it ranges from 28 to 87%, while the reference wind velocity ranges between 36 and 170 cm/sec.

B. Eulerian Correlation Function and Spectrum Function of Wind-Fluctuation in the Plant-Air Layer

Correlogram and spectral analysis techniques are convenient methods for specifying the character of turbulence in the plant-air layer.

In general, the Eulerian time correlation function is given by:

$$R_u(\sigma) = \frac{\overline{u'(t) \cdot u'(t+\sigma)}}{\overline{u'^2}} , \qquad (4.7)$$

where,

$u'(t)$, $u'(t+\sigma)$ are turbulent velocities at times t and $t+\sigma$, respectively,

$\sqrt{\overline{u'^2}}$ is the standard deviation of turbulent velocity.

On the other hand, the structure function defined as

$$B_{dd} = \overline{\left[u(x) - u(x+l)\right]^2}, \tag{4.8}$$

is usually used instead of the time correlation in the study of the micro-structure of turbulence. Taylor's hypothesis on the transformation from Eulerian time-correlation to Eulerian space-correlation is assumed to be applicable in the plant-air layer (which has a quite high turbulent intensity), so that,

$$l = \bar{u} \cdot \sigma$$

where $\bar{u}$, σ, l denote mean wind velocity, lag time, and separation distance, respectively. [The applicability of this hypothesis to atmospheric conditions has been confirmed both theoretically (Ogura, 1953; Gifford, 1956) and experimentally (Panofsky, 1958)].

By making use of the above relation, the following relation is obtained between Eulerian time-correlation and structure function,

$$B_{dd} = 2\overline{u'^2}\left\{1 - R_u(l)\right\}.$$

From the similarity theory of turbulence, the structure function for turbulence in the inertial subrange may also be given as,

$$B_{dd} = B_v^2 \cdot l^{2/3}, \tag{4.8a}$$

where B_v is the structure parameter defined by

$$B_v = C_1 \cdot \epsilon^{1/3}, \tag{4.9}$$

and ϵ is the rate of dissipation of turbulent energy. In the surface air-layer where the logarithmic wind profile holds, the dissipation rate is given by

$$\epsilon = \frac{V_*^3}{\kappa z} \tag{4.10}$$

where V_*, κ are friction velocity and von Karman constant, respectively.

The energy spectrum defining the contribution of the frequency range between n and (n+dn) to $\overline{u'^2}$ can be written as follows:

$$F(n) = 4\int_0^\infty R_u(\sigma)\cos(2\pi n\sigma)\,d\sigma, \qquad (4.11)$$

where F(n) is the energy spectrum function and n is the frequency. In the inertial subrange, the energy spectrum function can be determined only in terms of the dissipation rate, expressed as follows:

$$F(n) \propto \epsilon^{2/3} n^{-5/3}. \qquad (4.11a)$$

Eqs. (4.8a) and (4.11a) are the famous two-thirds and negative five-thirds power laws obtained from the similarity theory. The above two relations on the nature of the micro-structure of turbulence have been tested by many researchers (e.g., Perepelkina, 1959; Shiotani, 1953; Gurvich, 1960; Uchijima, 1959; Taylor et al., 1952) giving good agreement.

In order to examine the applicability of the similarity theory described above, Eulerian time-correlations, structure functions, and energy spectra have been computed from the 20 records of wind fluctuation in the plant-air layer.

The results shown in Table 4 include momental skewness, μ_3, kurtosis, μ_4, the structure paramter, B_v, the rate of dissipation of turbulent energy, ϵ, the smallest eddy size, λ_2, the largest eddy size, Λ_{xo}, the size of the energy-containing eddy, Λ_m, Eulerian space scale, L_u, skewness factor, S. F., flatness factor, F. F., intermittency factor, γ, and cross-correlation, $r_{(z_R \to z)}$.

An example of the structure function of the turbulent field in the plant-air layer is presented in Figure 8. The structure function from Eq. (4.8a) increases with separation distance. Also, the absolute value of the structure function is larger for the upper levels than for the lower levels. The dependence of the structure function upon the separation distance in the range of smaller distances shows good agreement with the straight line indicating the two-thirds power law. This agreement probably means that there is an inertial

TABLE 4.- The quantities relating to the micro-structure and statistical properties of turbulence in the corn plant-air layer.

Run	z (cm.)	B_v $cm^{2/3}.sec^{-1}$	ϵ $cm^2.sec^{-3}$	λ_2 cm.	Λ_{xo} cm.	Λ_m cm.	L_u cm.	$r_{130 \to z}$	μ_3	μ_4	S.F.	F.F.	γ
3	370	4.6	72.0	1.2		2200.0	348.8	0.23	0.0	2.7	-0.33	3.80	0.79
	130	3.7	37.6	1.4	361.2	328.3	48.2	1.00	1.4	6.2	0.58	6.23	0.48
	110	1.5	22.9	1.6			66.7	0.28	-0.07	5.5	0.02	6.81	0.44
	90	1.2	13.6	1.6			51.6	0.15	0.16	4.6	-0.34	4.61	0.65
	50	0.7	0.2	5.2	166.6	139.1	31.1	0.04	-0.45	2.2	-0.23	4.24	0.71
6	130	4.9	89.5	1.1	325.2	310.8	197.2	1.00	6.4	2.5	0.02	7.27	0.41
	110	2.1	6.7	2.1			81.1	0.63	2.5	13.2	0.37	5.81	0.51
	90	1.6	3.0	2.7			66.3	0.38	3.1	14.9	-0.89	9.13	0.33
	50	1.0	0.7	3.8	333.9	458.6	93.6	0.15	1.8	11.8	-1.49	9.23	0.32
7	130	10.1	763.2	0.7	541.8	547.4	543.9	1.00	0.5	1.9	0.08	4.38	0.68
	110	7.4	298.7	0.9			185.2	0.71	1.8	6.7	0.75	7.36	0.41
	90	6.0	160.4	1.0			136.6	0.38	2.7	18.9	0.99	16.69	0.18
	50	5.7	140.6	1.0		53.1	92.5	0.29	2.6	15.7	1.16	14.73	0.20
10	130	-	-	-									
	110	9.5	651.4	0.7			118.9		1.8	8.6	-0.06	9.05	0.33
	90	5.7	141.3	1.0			165.3		4.2	8.3	0.41	7.81	0.38
	50	5.6	131.1	1.0			50.5		1.6	6.3	-0.24	12.59	0.23
16	130	7.8	352.9	0.8	325.7	340.3	50.1	1.00	1.4	4.3	-0.10	6.72	0.45
	110	7.8	16.8	1.7			56.6	0.55	1.7	8.2	-0.10	5.12	0.58
	90	2.8	16.8	1.7			54.7	0.43	0.7	3.6	0.32	11.02	0.27
	50	2.3	8.8	2.0	283.2	249.9	41.0	0.31	1.3	6.5	-0.07	9.45	0.32

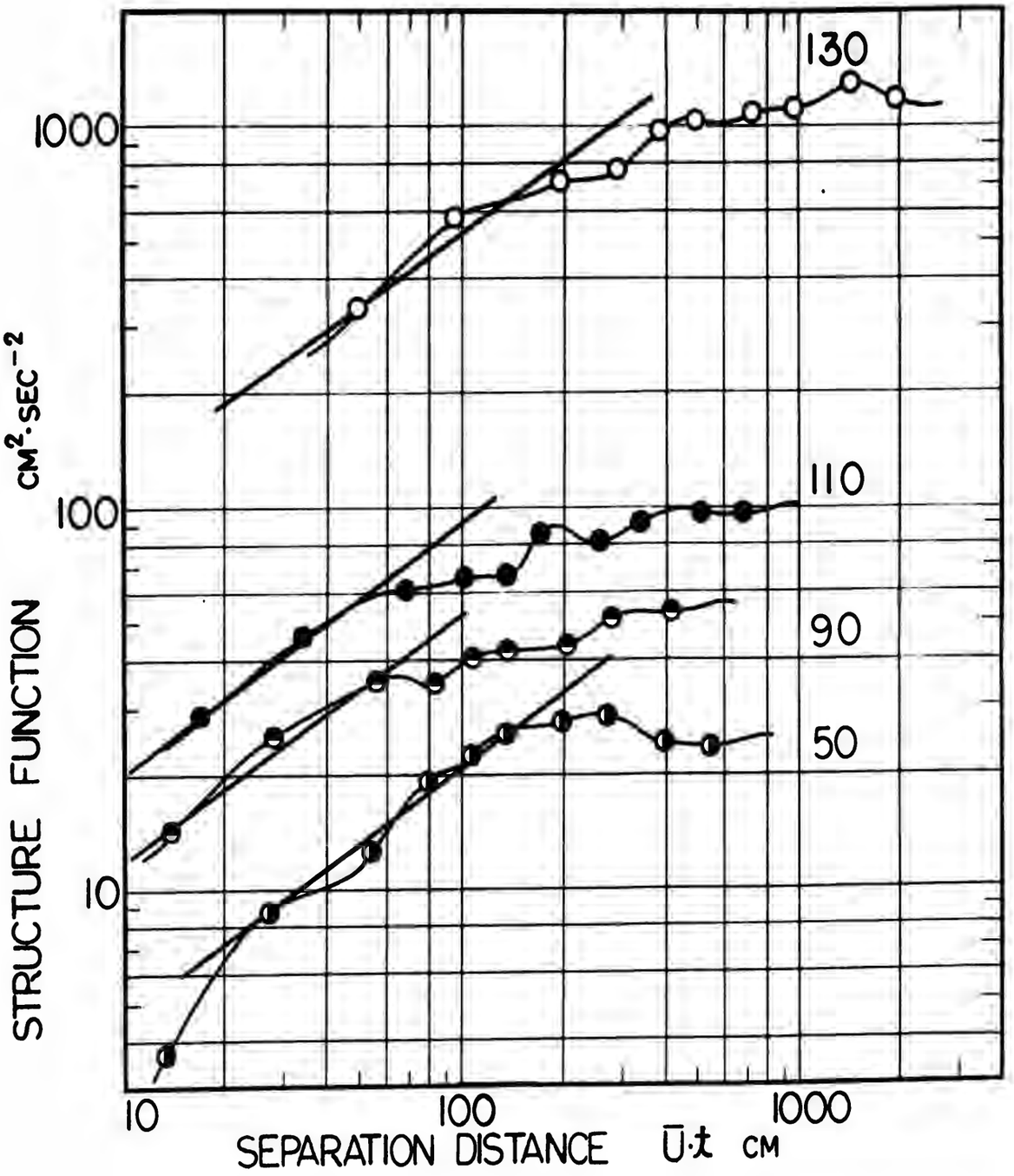

FIG. 8. STRUCTURE FUNCTION. (RUN 6)

subrange of turbulence in the plant-air layer to which the similarity theory can be applied. This result agrees well with that of Nakagawa's study on airflow in a paddy.

As can be seen in Table 4, the structure parameter, B_v , governing the turbulent velocity, decreases with increasing depth (H-z) from 3.7 ~10.1 at a height of 130 cm. to 0.7 ~5.7 at a height of 50 cm. Also, the structure parameter increases with increasing reference wind velocity. The value of the parameter in the upper layer is larger than that (2.0 to 3.0 $cm^{2/3}$/sec.) for a surface air layer.

Generally, the rate of dissipation of turbulent energy is approximately given by

$$\epsilon = K\left(\frac{d\bar{u}}{dz}\right)^2, \tag{4.12}$$

where K is the exchange coefficient.

Using Eq. (4.12) and the empirical relation (3.11) for the friction velocity in the plant-air layer, the above relation becomes

$$\epsilon = \frac{V_{*H}^3}{l(z)} e^{-8.4\left(1-\frac{z}{H}\right)} \qquad z \le H \tag{4.12a}$$

Substituting the above relation into Eq. (4.9) gives

$$B_v = \frac{C_1 \cdot V_{*H}}{[l(z)]^{1/3}} e^{-2.8\left(1-\frac{z}{H}\right)} \qquad z \le H \tag{4.13}$$

This equation indicates that the structure parameter in the plant-air layer depends mainly on terms such as the exponential relation for the friction velocity, $V_{*H} e^{-2.8\left(1-\frac{z}{H}\right)}$, the mixing length profile, $l(z)$, and the friction velocity at the upper boundary of the plant-air layer. From a comparison of the two quantities, B_v and ϵ, it is found that the decrease in the dissipation rate within the plant-air layer is steeper than the decrease of the structure parameter.

The values of the structure parameter obtained from the measurement of wind-fluctuation are compared in Figure 9 with those calculated from Eq. (4.13) using the data on friction velocity and mixing length in the plant-air layer. It is evident from Figure 9 that the structure parameters calculated by the semi-empirical formula are in good agreement with those obtained from wind-fluctuation measurements. This fact, plus the fact that the structure function can be approximated by the two-thirds power law, implies that the results derived from the similarity theory of turbulence, with some modifications for fundamental quantities, V_* , $\ell(z)$, etc., are applicable even to the plant-air layer in which momentum absorption occurs.

One example of the vertical distributions in and above the corn plant-air layer: the structure parameter, B_v; the dissipation rate of turbulent energy, ϵ; the size of the largest eddy, Λ_{xo}; and the size of the smallest eddy, λ_2: is presented in Figure 10. The results obtained from Eqs. (4.12a) and (4.13) are presented as curves in this figure. On the other hand, the results from Eqs. (4.8a) and (4.9) are presented as points.

The size of the smallest eddy is defined by,

$$\lambda_2 = 15\left(\frac{\nu^3}{\epsilon}\right)^{1/4}, \qquad (4.14)$$

where ν is the kinematic viscosity of air (equal to 0.14 $cm^2/sec.$). According to MacCready (1953), this is the size of eddy below which 90% of the viscous dissipation occurs. Thus, this size may show the critical eddy size between the inertial and viscous subranges of turbulence.

As shown in Figure 10, the decrease of the structure parameter with depth into the plant layer is more gentle than that of the dissipation rate. This indicates good agreement between the measured points and the curves predicted by Eqs. (4.12a) and (4.13). The value of the dissipation rate, on which the statistical characteristics of turbulence within the inertial subrange depend,

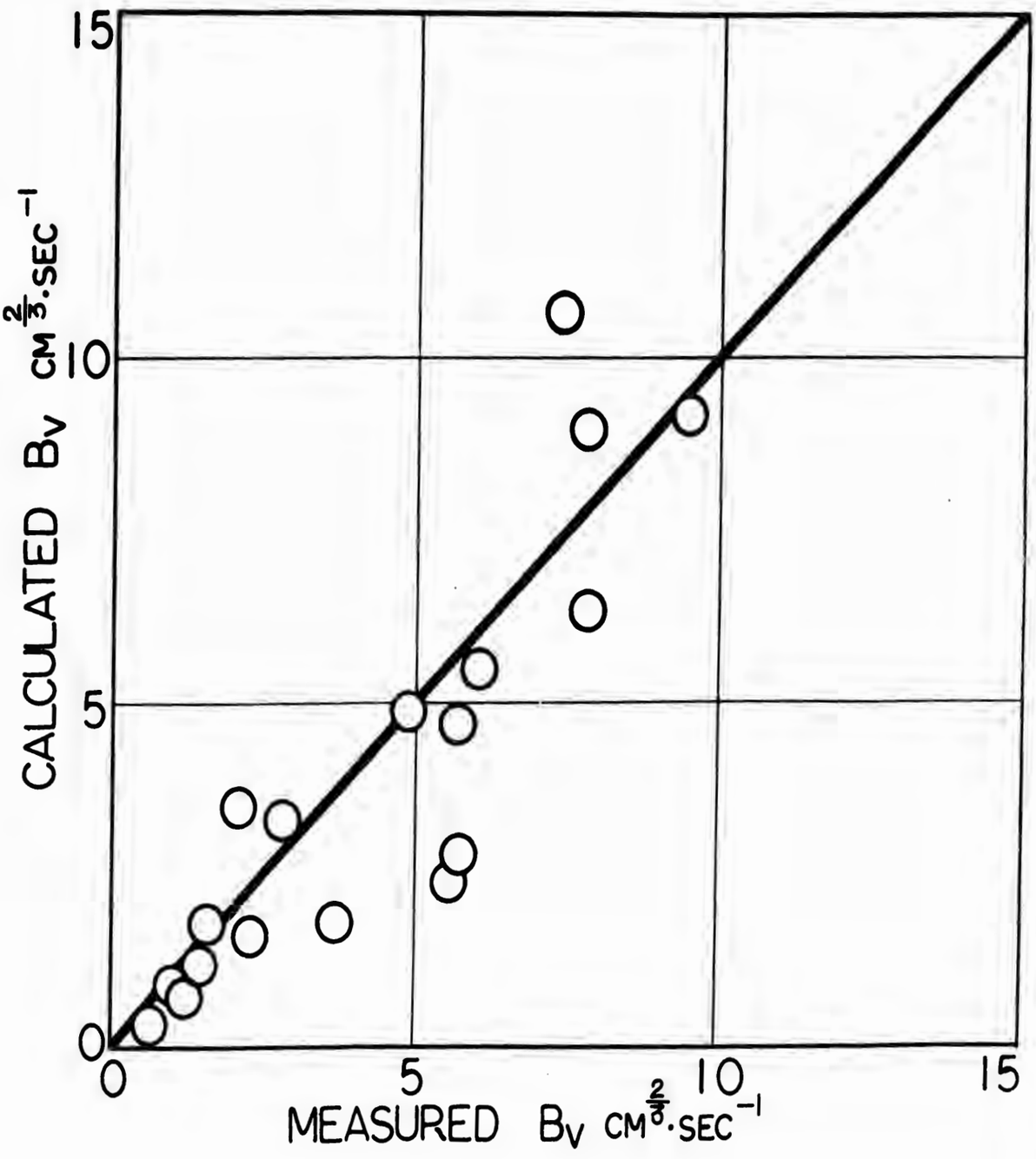

FIG. 9. COMPARISON OF CALCULATED B_V WITH MEASURED B_V.

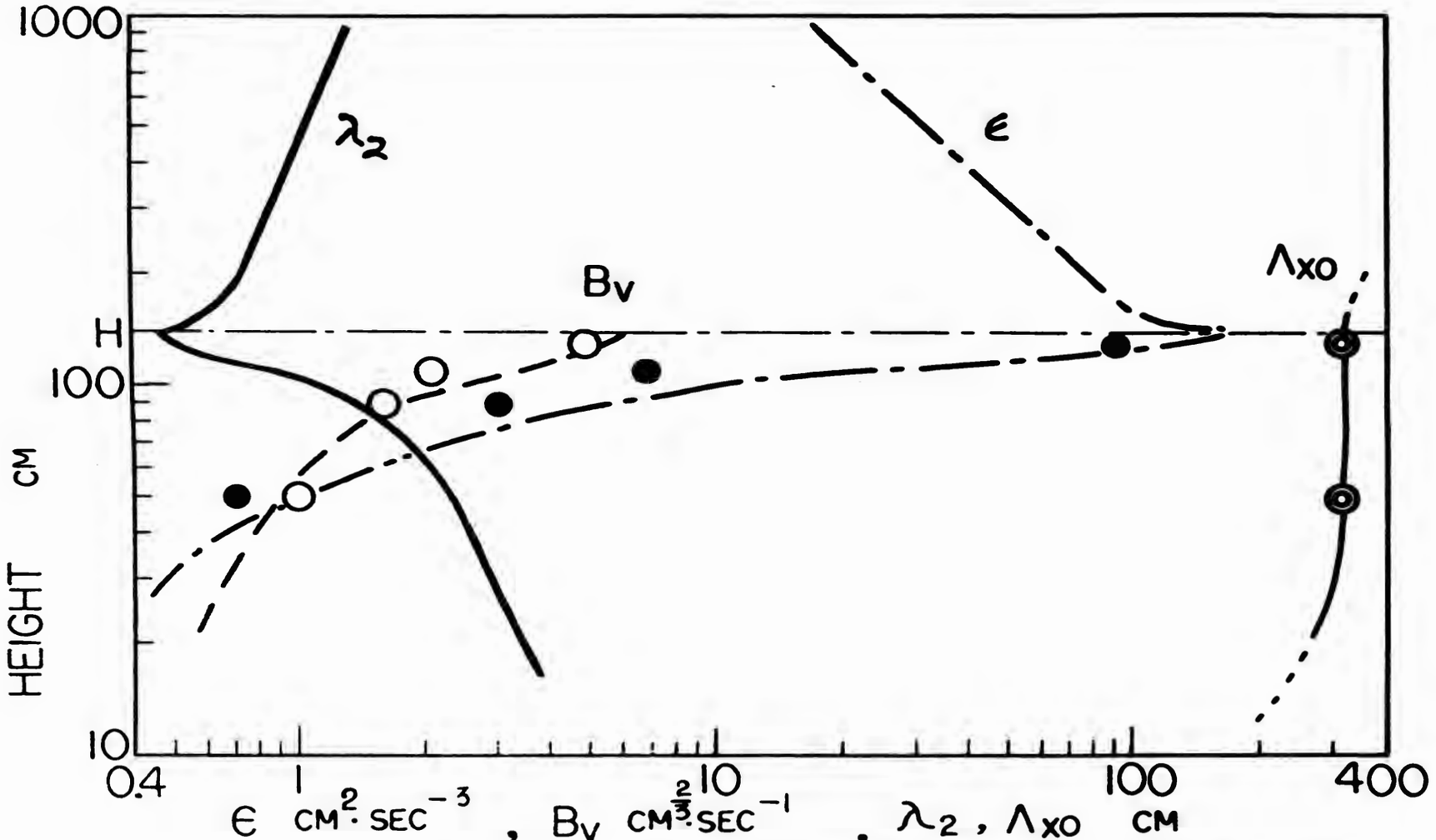

FIG. 10. VERTICAL PROFILES OF DISSIPATION RATE, STRUCTURE PARAMETER, SMALLEST EDDY, LARGEST EDDY. (RUN 6)

shows a maximum of about 200 $cm^{2/3}$/sec. at the upper boundary of the layer. It decreases rapidly with increasing distance above and below this boundary level. The difference in the dissipation rate in and above the plant layer is due to decreased momentum flux within the plant-air layer.

The total dissipation, E (ergs/cm^2·sec.), is obtained from the vertical distribution of the dissipation rate, ϵ, within the entire plant-air layer, ($0 \leq z \leq H$) as,

$$E = \int_0^H \rho \epsilon \, dz = \rho \int_0^H \frac{V_{*H}^3}{l(z)} e^{-8.4\left(1-\frac{z}{H}\right)} dz \qquad (4.15)$$

E is important in the study of momentum and heat balances in plant-air layers because it represents the decay of the major portion of energy into heat. Values of E obtained by graphical integration are presented in Table 5.

TABLE 5.- The total dissipation amount, E, in the corn plant-air layer.

Run	3	6	7	10	16
U_H cm/sec.	36	78	150	169	95
E ergs/cm^2·sec.	2.5	6.9	40.2	36.7	17.5

As can be seen in this table, the total dissipation, E, increases rapidly (proportional to the third power of $\overline{U}_H$). It nonetheless can be safely concluded that the values of E are negligibly small in comparison with the main heat budget items (e.g., net radiation, sensible and latent heat flux, etc.)

The minimum size of the smallest eddy occurs at the boundary surface of the plant-air layer where maximum energy dissipation is observed. It increases with distance on either side, following the exponential law in the plant layer and the one-third power law in the surface air layer. The size of the largest eddy defining the critical eddy size in the lower frequency range is presented

also in Figure 10 and Table 4. To find the size of the largest eddy in the inertial subrange, the energy value of each frequency multiplied by $n^{5/3}$ was plotted against the frequency. Therefore, the inertial subrange of turbulence is represented by the horizontal straight line on this graph. The size of the largest eddy was estimated from the critical frequency, n^*, at which the relation between $n^{\frac{5}{3}} \cdot F(n)$ and n deviated from the horizontal straight line showing $F(n) \propto n^{-\frac{5}{3}}$. Thus,

$$\Lambda_{x0} = \frac{1}{n^*} \overline{u}_z \quad , \tag{4.16}$$

where Λ_{x0} is the size of the largest eddy and $\overline{u}_z$ is the mean wind velocity. Both Figure 10 and Table 4 show that the size of the largest eddy in the plant-air layer does not change appreciably with height above the ground surface. Furthermore, it is nearly equal in size to the energy containing eddy, Λ_m. The largest eddy is four times larger than the height above the ground surface. (The size of the energy containing eddy was defined as the eddy size corresponding to the characteristic frequency at which the maximum fraction of turbulent energy was observed [see Figure 11,b].) Using the results of his spectral analysis of the vertical wind components in a surface air layer over a level field, Gurvich (1960) has shown that the frequency corresponding to the largest eddy is two times larger than that of the energy containing eddy.

Using Eq. (4.10) and the Eulerian time-correlation functions, nine spectra, including one from 370 cm., four from 130 cm., and four from 50 cm., have been worked out to obtain the characteristics of the energy distribution at each frequency and the effects of the plant-air layer upon the energy distribution. The spectra for each run are shown in Figure 11-a as plots of F(n) vs. log-n. The frequency range predicted by the power law is expressed approximately by a straight line. The value of the frequency, n, was generalized by multiplying by $z/\overline{u}_z$.

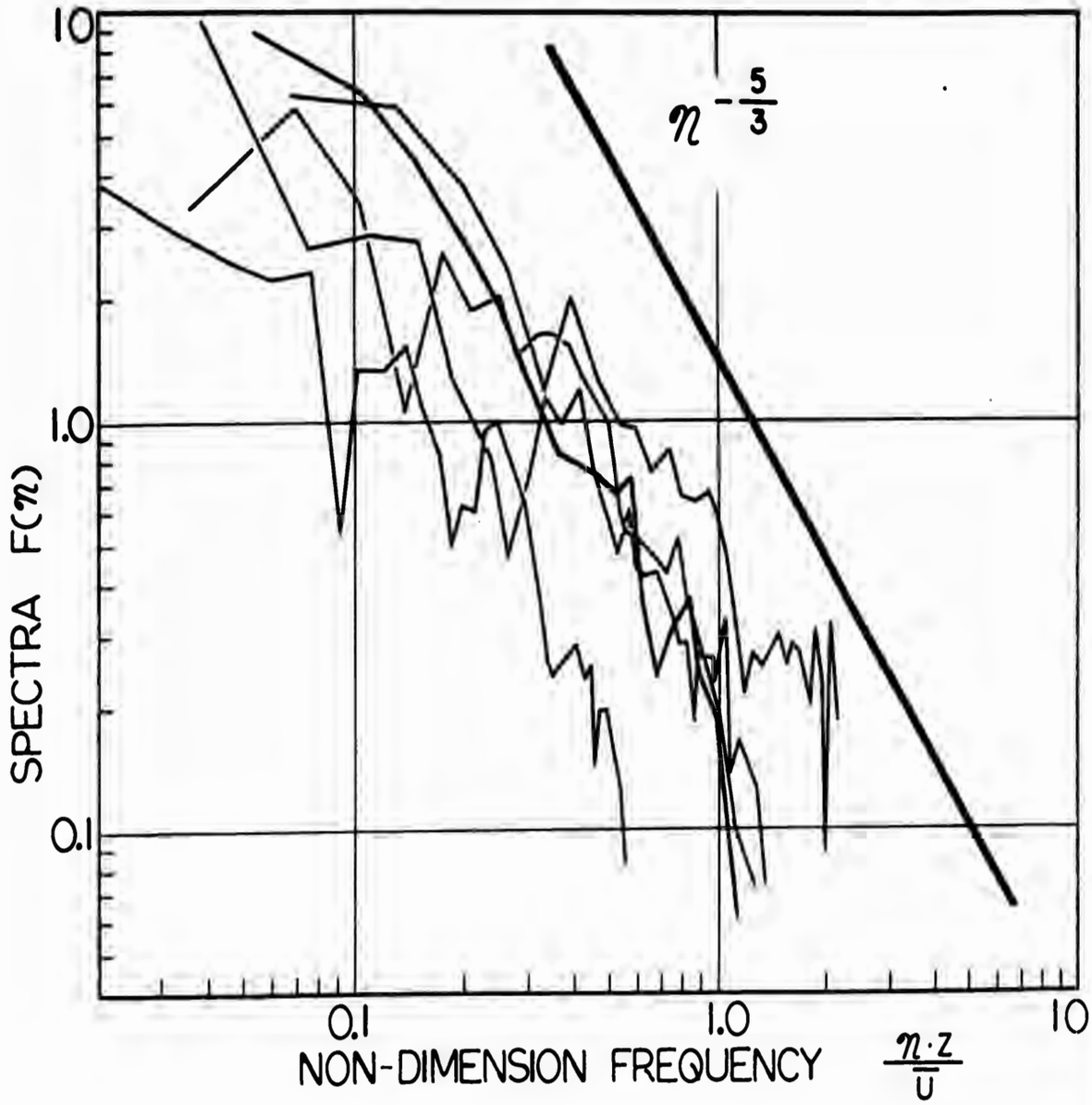

FIG. 11-A. SPECTRA OF WIND VELOCITY.

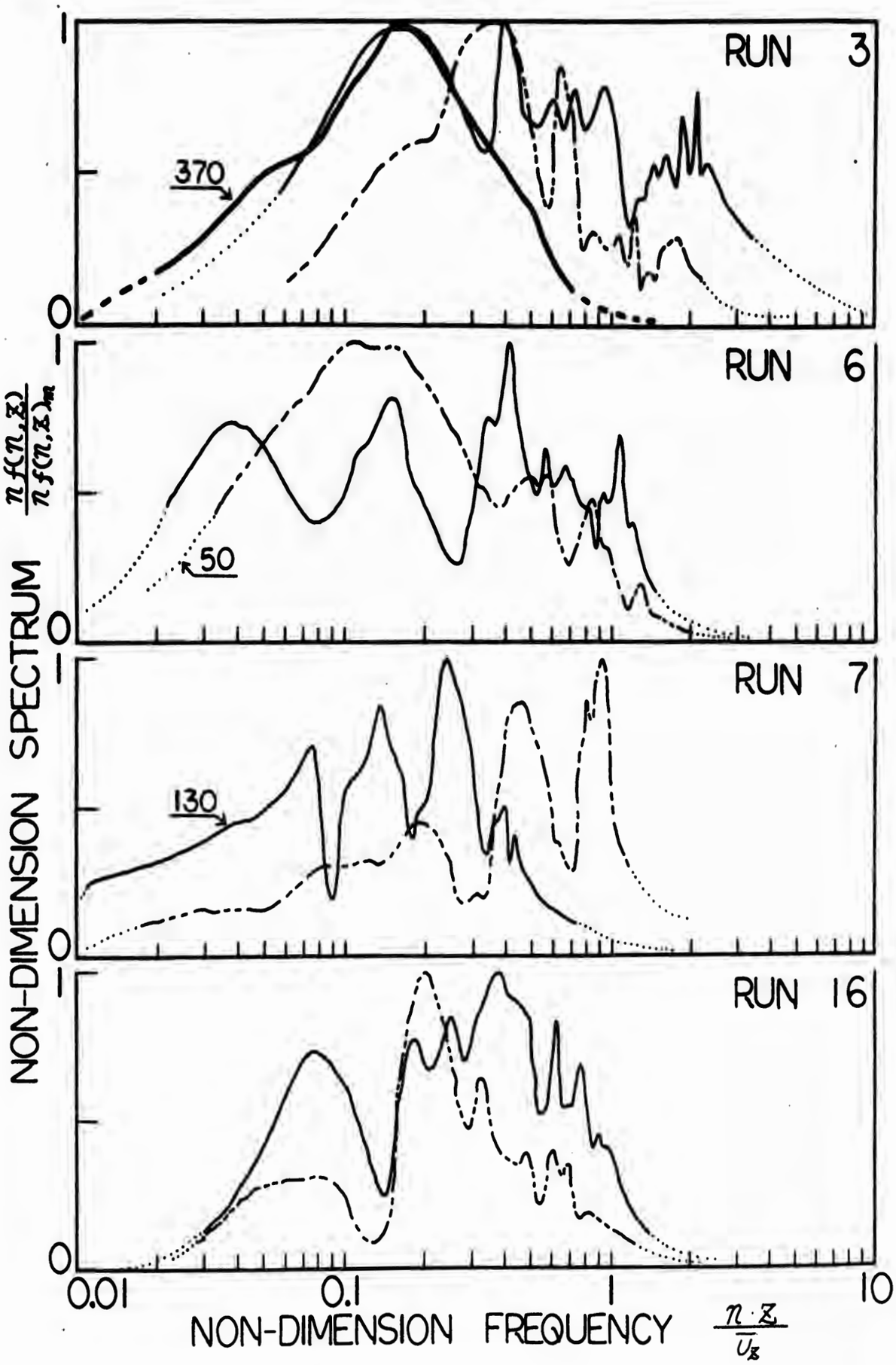

FIG. 11-B. SPECTRA OF WIND VELOCITY.

As shown in Figure 11-a, the spectral curves are considerably more ragged than those customarily obtained from the turbulent field of a surface air-layer. But it may still be stated that the general tendency of decreasing energy with decreasing frequency agrees with the negative five-thirds power law of the similarity theory of turbulence. The excessively ragged nature of the spectral curves seems to result from the selective absorption and addition of turbulent energy at certain characteristic frequencies.

It is difficult to intuitively obtain information about the energy spectrum from Figure 11-a. Therefore, the spectra for each run are shown also in Figure 11-b as plots of $nF(n)$ vs. log-n. The area under the curve represents the amount of energy contributing to the total turbulent energy ($\overline{u'^2}$). The value of the turbulent energy was generalized by,

$$\frac{nF(n)}{nF(n)_{max}},$$

where $nF(n)_{max.}$ denotes the amount of turbulent energy of the maximum-energy containing eddy.

As can be seen in Figure 11-b, the curve for the 370 cm. height shows a well-defined peak at $\frac{n.z}{\bar{u}_z} = 0.16$, i.e,. at a period of about 35 sec. The distribution curve is smooth. On the contray, the curves for the 130 cm., and the 50 cm. heights (in the plant-air layer) distinctively show an unusually irregular distribution. It is evident from a comparison of the spectra for the 130 cm. and 50 cm. heights that there is no clear correlation between them, and the mutual difference, particularly in the higher frequency range, increases with wind velocity. In Run 7 with a wind velocity of 150 cm/sec., a considerable difference was observed between the energy spectrum of both heights. That is, the spectrum for the 130 cm. height has relatively more energy in the dimensionless frequency range of 0.01 to 0.5 than does the spectrum for the 50 cm. height, while the latter spectrum mainly contributes in the range of 0.35 to 1.5.

In the case of Run 3, with its lower wind velocity of 36 cm/sec., it is possible to find good agreement between spectra for the 370 cm. and 130 cm. heights at frequencies less than $\frac{n \cdot z}{\bar{u}_z} = 0.35$. The energy spectrum for 130 cm. appears as if a new turbulent field consisting of fine fluctuations were superimposed on that for 370 cm. The complicated nature of the energy spectrum for the turbulent field in the plant-air layer compared with that for a surface air-layer should be attributed to the modification of the turbulent field by both energy dissipation and the interaction between air-flow and plant bodies. In particular, the main reason for the marked difference in the energy spectra at high wind velocities may reasonably be attributed to the stirring of the air-flow by the waving and fluttering of the plant bodies. Although the exact relationship is uncertain, it is likely that the peculiar periodicity of the energy distribution curve corresponds to a periodicity of the waving and fluttering of the plant bodies. The facts described above imply that plant bodies effect air flow in the same way as do turbulence generating grids with complicated flexibility. In order to obtain a better understanding of the physical nature of the turbulent field in plant-air layers, it is hoped that further investigations will be performed both theoretically and experimentally on the air-flow within flexible, turbulence-creating grids.

The characteristic length scale, namely the Eulerian space scale, in the longitudinal direction of wind velocity is given by,

$$L_u = t_u \cdot \bar{u}_z = \bar{u}_z \int_0^\infty R_u(\sigma)\, d\sigma , \qquad (4.17)$$

where L_u , t_u denote the Eulerian space and time scales, respectively. This scale is considered to be a measure of the magnitude of the lumps of fluid which move together as a unit. The values of the Eulerian space scale obtained using (4.17) are presented in Table 4. At lower wind velocities, the Eulerian space scale in the plant-air layer increases gradually with increasing height

above ground surface and is in the range from 31 to 66 cm. With increasing wind velocity, the Eulerian space scale, particularly in the upper part of the layer, increases greatly. Also, the vertical profile of the space scale is steep in the plant-air layer. These results for the corn plant-air layer differ from those for a paddy field (Nakagawa, 1956). The Eulerian space scale reported by Nakagawa for a paddy field (H=90 cm.) has a nearly constant vertical profile and is larger than that for a cornfield (H=140 cm.) On the other hand, the results for the corn plant-air layer agree well with results obtained for a plant-air layer by Stoller and Lemon, (1963) and Wright and Lemon, (1962). The condition described above implies that the longitudinal scale of the largest turbulent eddy in the plant-air layer is lengthened with increasing wind velocity. This result agrees well with that for the largest eddy in a surface air layer (Shiotani, 1953).

C. On the Anisotropy of Turbulence in the Plant-Air Layer

Generally speaking, it is well known that the following condition for isotropic turbulence does not hold in a surface air layer,

$$\overline{u'^2} = \overline{v'^2} = \overline{w'^2},$$

where u', v', w' denote the three components of the turbulent velocity. From measurements of wind fluctuation over a level snow field, Shiotani, (1953) reported that the coefficient of anisotropy ranged from 0.095 to 0.41, decreasing with increasing wind velocity. This coefficient is defined by,

$$a_L = \frac{\Lambda_{z0}}{\Lambda_{x0}},$$

where Λ_{z0} and Λ_{x0} denote the vertical and horizontal scales of the largest eddy, respectively.

Referring to the results obtained experimentally by Perepelkina, (1957) and Gurvich, (1960) Monin, (1962) has shown the following mean value for the coefficient of anisotropy in a surface air layer, $a_V = \frac{\sigma_w}{\sigma_u} = 0.3,$

where σ_u, σ_w denote the root mean squares of the horizontal and vertical components of turbulent velocity, respectively. This mean value is well-supported by the results ($a_v = 0.35$) of Shiotani (1953). The experimental facts mentioned above clearly indicate that turbulence in a surface air layer is considerably anisotropic both in scale and in turbulent energy. However, there are no experimental results available to indicate whether turbulence in plant-air layers is isotropic or not. Supposing that relatively steady turbulence with fine-fluctuations is approximately isotropic, Stoller and Lemon, (1963) used the Eulerian space scale in the longitudinal direction for evaluating the exchange coefficient in the corn plant-air layer. Even if isotropic turbulence does exist in the steady fine fluctuations, there seems to be a question of whether the exchange coefficient so evaluated is representative of the turbulent field in the layer, because the exchange coefficient applicable in evaluating the mean vertical flux of each quantity is mainly determined by the largest representative eddy in a given turbulent field.

As pointed out by Lettau, (1952), in the study of anisotropy of the turbulent field of the plant-air layer, it is more reasonable to consider the four parameters,

$$l_w,\ l_u,\ \sqrt{\overline{u'^2}},\ \sqrt{\overline{w'^2}},$$

and the two coefficients of anisotropy

$$a_v = \frac{\sqrt{\overline{w'^2}}}{\sqrt{\overline{u'^2}}}, \qquad a_L = \frac{l_w}{l_u}, \tag{4.18}$$

where, l_w, l_u denote the vertical and horizontal scales of the largest representative eddy in a turbulent field,

a_v, a_L denote the coefficients of anisotropy calculated from considering turbulent velocity and eddy scale, respectively.

In evaluating the eddy scale coefficient of anisotropy in the plant-air layer, the following method was applied. As described earlier, the turbulent velocity

in the plant-air layer is given by,

$$\sqrt{\overline{u'^2}} = \frac{C_1}{\sqrt{2}}\left[\frac{l^*}{l(z)}\right]^{1/3} V_{*H}\, e^{-2.8\left(1-\frac{z}{H}\right)} .$$

This relation indicates that the turbulent velocity, $\sqrt{\overline{u'^2}}$, depends upon the ratio, $\frac{l^*}{l(z)}$ which characterizes the eddy scale coefficient of anisotropy. The horizontal scale, $l^* \simeq l_u$, as defined above is similar in nature to the horizontal scale of the largest turbulon proposed by Inoue, (1952) as,

$$R_u(\sigma) = 1-\left(\frac{\sigma}{T_{x0}}\right)^{2/3},$$

$$\Lambda_0 = T_{x0}\cdot \bar{u} \quad ,$$

where T_{x0} is the passing time of the largest turbulon.

Using the following assumption,

$$\left(\frac{l^*}{l(z)}\right) = \frac{l_u}{l_w} \simeq 1 ,$$

the results calculated from Eq. (4.19) are compared with those measured in the plant-air layer, (Figure 12).

If isotropic turbulence exists in the plant-air layer, the points will be on the straight line. However, Figure 12 (top) shows a markedly systematic departure of points from the straight line, particularly for large turbulent velocities (which occur at high wind velocities). In order to characterize this fact in more detail, the eddy scale coefficient of anisotropy, a_L, was determined by,

$$a_L = \frac{l_w}{l_u} = \left[\frac{\left(\sqrt{\overline{u'^2}}\right)_c}{\left(\sqrt{\overline{u'^2}}\right)_m}\right]^3 , \qquad (4.19)$$

where $\left(\sqrt{\overline{u'^2}}\right)_m$, $\left(\sqrt{\overline{u'^2}}\right)_c$ denote the measured turbulent velocity and turbulent velocity calculated by Eq. (4.5) assuming isotropy, respectively. The result at a height of 130 cm. so obtained is presented in Figure 12 (bottom).

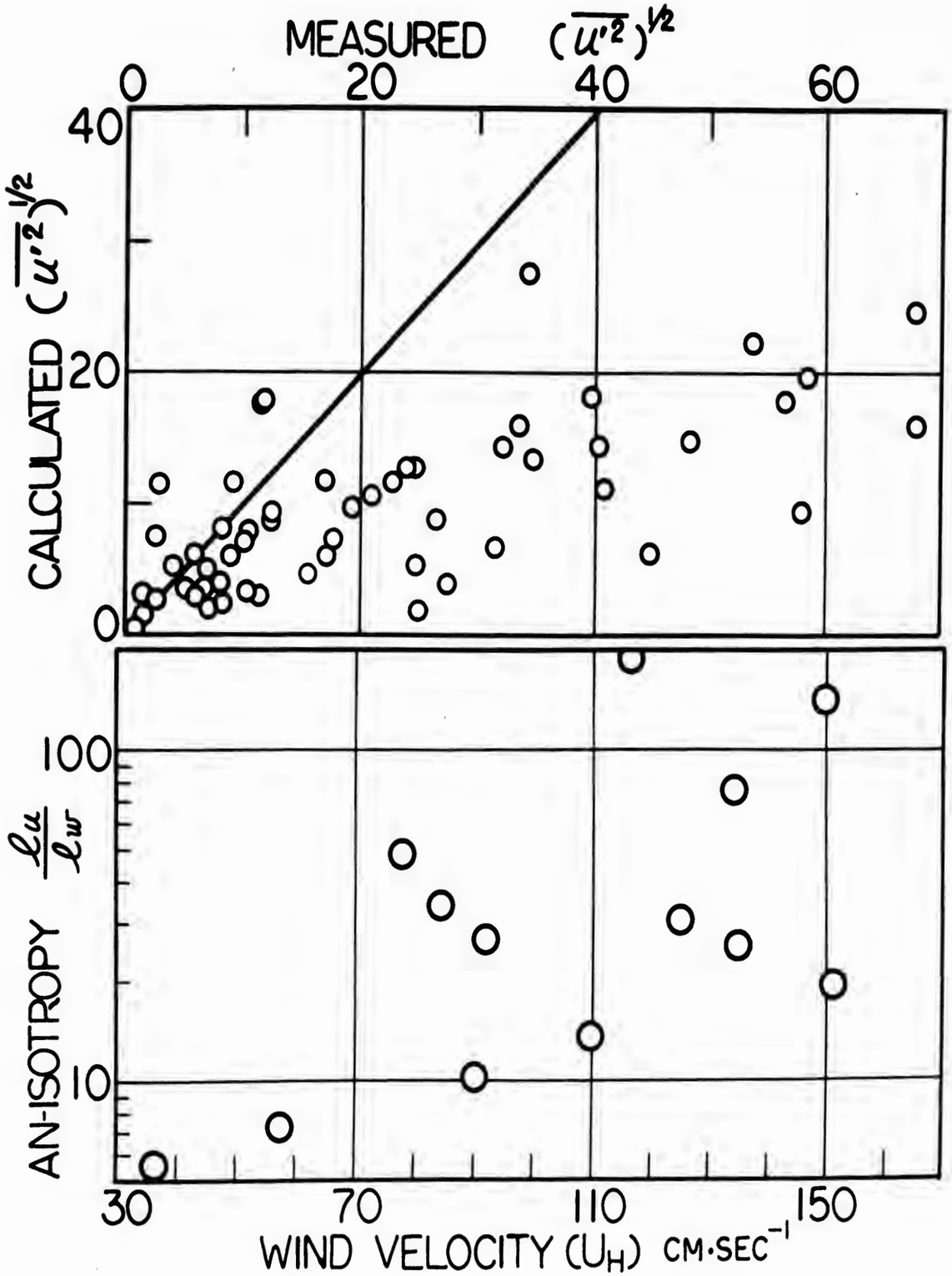

FIG. 12. COMPARISON OF CALCULATED $(\overline{u'^2})^{1/2}$ WITH MEASURED (TOP), DEPENDENCE OF ANISOTROPY ON WIND VELOCITY.

As seen in this figure, the coefficient of anisotropy, a_L , decreases remarkably with increasing wind velocity from about 0.2 at a wind velocity of 36 cm/sec. to 0.01 at 150 cm/sec. Similar results also were attained by comparing the Eulerian space scale with the mixing length. The ratio of the mixing length to the Eulerian space scale at the 130 cm. height decreases as the reference wind speed increases, ranging from 0.42 at 36 cm/sec. to 0.04 at 150 cm/sec. But the values for the 50 cm. height range from 0.66 to 0.217. The results in Figure 12 indicate that the largest eddy should have the shape of an oblate spheroid.

The turbulent velocity coefficient of anisotropy, a_V , is shown in Figure 13. This coefficient is evaluated by,

$$a_V = \frac{\sqrt{\overline{w'^2}}}{\sqrt{\overline{u'^2}}} \simeq \frac{0.85\, V_*}{\sqrt{\overline{u'^2}}} \quad . \tag{4.20}$$

Figure 13 shows that the turbulent velocity coefficient of anisotropy depends upon wind velocity and height above ground surface. Under conditions of low wind (left), the coefficient increases from 0.6 at the upper boundary surface to 0.85 at the 50 cm. height. We conclude from the results of this figure that the turbulence in the lower part of the plant-air layer is approximately isotropic concerning the turbulent velocity. The values of a_V in the plant-air layer are relatively larger than those (a_V = 0.3) which are observed in the surface air-layer above the plant canopy. With increasing wind velocity (right), the coefficient, a_V , decreases, particularly at the lower levels, and approaches the value for a surface air-layer.

From the results described above, it can safely be concluded that the turbulent field in the plant-air layer is anisotropic with respect both to turbulent velocity and eddy scale. This suggests that one has to use both the vertical component of turbulent velocity, $\sqrt{\overline{w'^2}}$, and the vertical eddy scale, $l_w = l(z)$, that is, the vertical mixing length, in determining the vertical exchange coefficient for plant-air layers.

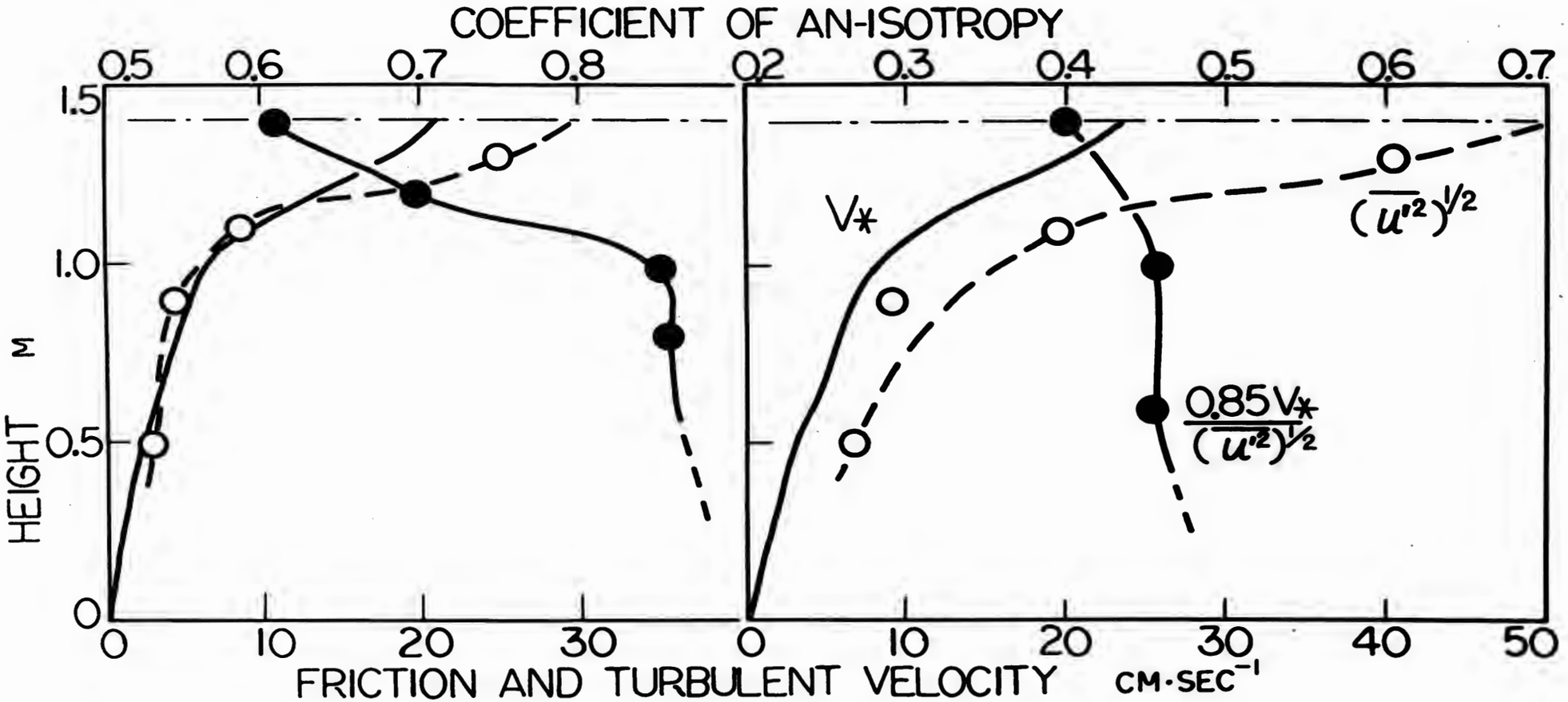

FIG. 13. VERTICAL PROFILES OF COEFFICIENT OF ANISOTROPY, FRICTION AND TURBULENT VELOCITIES.

D. Statistical Properties of Wind Fluctuation in the Plant-Air Layer

In the three preceding sections, the discussion has centered around the characteristics of the micro-structure of turbulence in the plant-air layers. However, statistical properties, particularly the probability density, of wind fluctuations are important quantities. Their meanings are readily understood and are relevant to the basic mechanical processes of the motion of air flow. As pointed out by Frenkiel, (1951) and Imai, (1962), cup anemometer and hot-wire anemometer results can be expressed as functions of the horizontal component of wind velocity, as

$$V_H = \left\{(\bar{u} + u')^2 + v'^2\right\}^{1/2},$$

where,

V_H, $\bar{u}$, u', and v' denote the wind velocity measured by the anemometer, mean wind velocity in the mean wind direction, the longitudinal component, and the perpendicular component of turbulent velocity, respectively.

At small turbulent intensities, the following relation may reasonably be used for determining the mean wind velocity,

$$V_H \simeq \bar{u} + u',$$

because the difference between the perpendicular and longitudinal components is negligibly small. On the other hand, at high turbulent intensities such as those observed in a surface air-layer or plant-air layer, this difference is no longer negligible. Assuming that each turbulent component has a normal distribution, Frenkiel and Imai have proposed approximate formulae for obtaining the correct mean wind, $\bar{u}$, the correct turbulent intensity, $\frac{\sqrt{\overline{u'^2}}}{\bar{u}}$, and the joint distribution curve which differs from a normal distribution curve.

Although the theoretically obtained facts are of great importance in studying the probability density of wind-fluctuation within the plant-air layer, experimental data about the anisotropy of the horizontal turbulent velocities are not available. For the sake of simplicity, the following inequality was used as a first approximation,

$$u' \gg v'.$$

For information about the statistical properties of wind-fluctuation in the plant-air layer, several statistical quantities such as cross-correlation, momental skewness, kurtosis, skewness, and flatness factors, and the intermittency factor were determined from the wind-fluctuation records. Sampling durations of 10 minutes and observational intervals of 1 second were used except for the cross-correlation. The cross-correlation of the wind fluctuation between two heights was computed from the data of 4-minute periods extracted at 1-second intervals. The following formulae were used in determining the above mentioned statistical quantities;

$$\begin{aligned}
r_{130\to z} &= \overline{u'_{130} \cdot u'_z} \Big/ \sqrt{\overline{u'^2_{130}}} \cdot \sqrt{\overline{u'^2_z}}, \\
\mu_3 &= \overline{u'^3} \Big/ \left(\overline{u'^2}\right)^{3/2}, \\
\mu_4 &= \overline{u'^4} \Big/ \left(\overline{u'^2}\right)^2, \qquad (4.21) \\
\text{S.F.} &= \overline{\{u(t)-u(t+\sigma)\}^3} \Big/ \left[\overline{\{u(t)-u(t+\sigma)\}^2}\right]^{3/2}, \\
\text{F.F.} &= \overline{\{u(t)-u(t+\sigma)\}^4} \Big/ \left[\overline{\{u(t)-u(t+\sigma)\}^2}\right]^2, \\
\gamma &= 3.0 \Big/ \text{F.F.},
\end{aligned}$$

where $r_{130\to z}$, μ_3, μ_4, S. F., F. F., and γ denote the cross-correlation, momental skewness, kurtosis, skewness factor, flatness factor, and intermittency factor, respectively. The other notations have their usual meanings.

The results obtained from these definitions are shown in Table 4. Almost all the values of momental skewness, μ_3, are "positive". Momental skewness is a measure of the departure of the velocity frequency distribution from a symmetrical distribution. A positive value indicates that the frequency distribution curve falls off rapidly in the lower wind regions and tails off gradually at the higher wind regions. At the lowest wind velocity (Run 3), small negative momental skewness values were observed in the lower part of the plant-air layer.

In spite of the scatter in the values of μ_3 and μ_4, it can be seen that the two vary differently with wind velocity in the zone between the upper (130 cm.) and lower (50 cm.) parts of the plant-air layer. That is, the momental skewness, μ_3, for the lower level increases gradually from -0.4 at 36 cm/sec. to 2.0 at 160 cm/sec., while at the upper level it decreases slightly from 1.5 to 0.45. Kurtosis, μ_4, at the lower level shows a remarkable increase with wind speed, changing from the platykurtic distribution to the leptokurtic, but μ_4 at the upper level displays a quite different character.

The above facts seem to indicate that increasing wind velocity influences the frequency distribution of wind fluctuation differently at the upper and lower levels of the plant-air layer. In the upper part, a high wind velocity brings on a nearly symmetric and uniform distribution of wind fluctuation due to vigorous mixing of air particles, but an asymmetric and leptokurtic distribution results in the lower part from a mixing of air particles of higher velocity into the calm air-layer. However, under low wind conditions, large fluctuations in the surface air layer do affect the wind fluctuation in the upper part, but do not appreciably affect the wind fluctuation in the lower part.

Figures 14-a and 14-b show two segments of the wind fluctuation record for heights at 370, 130, and 50 cm. (Runs 3 and 7) obtained at the Ellis Hollow cornfield.

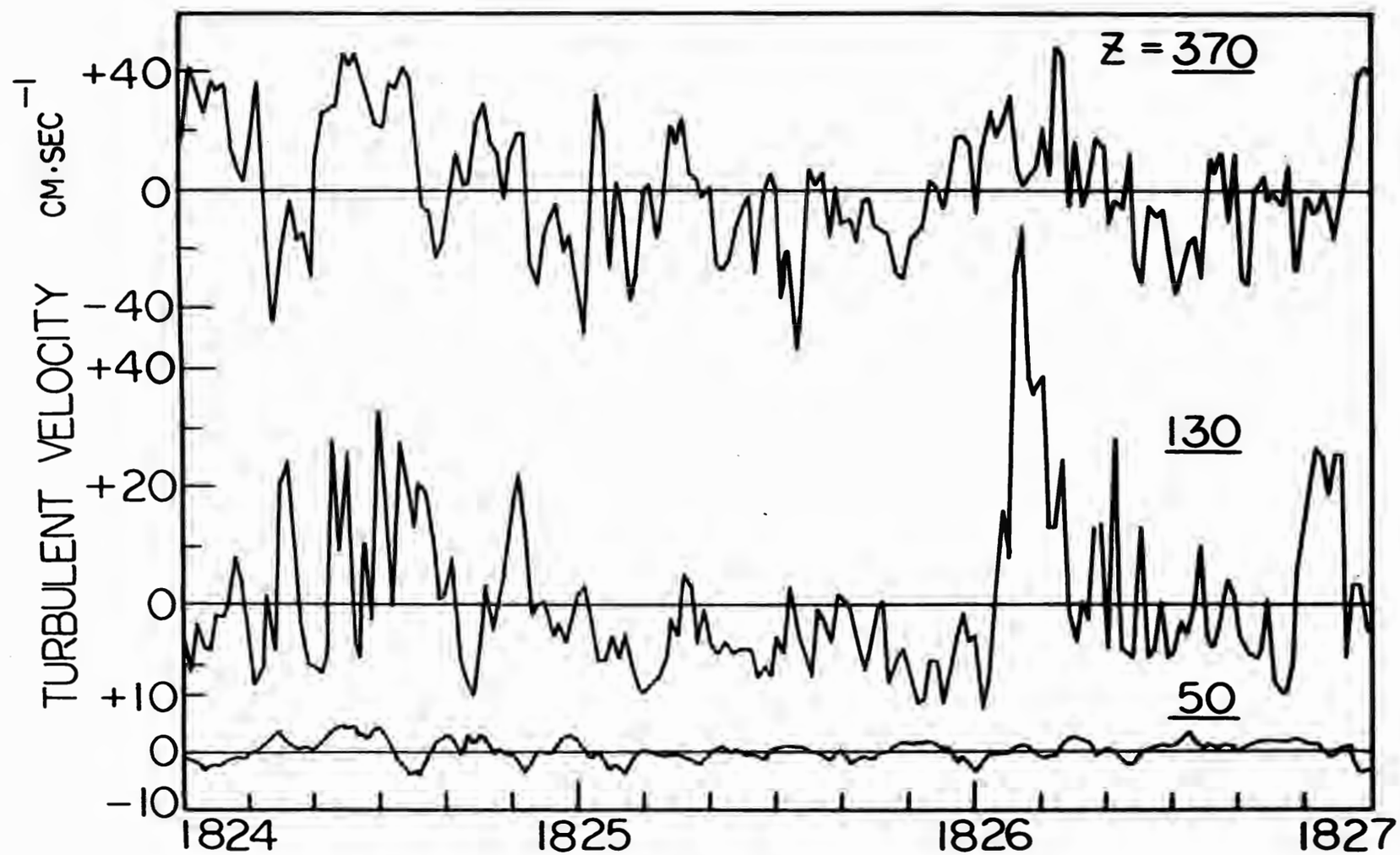

FIG. 14-A. WIND VELOCITY FLUCTUATION(RUN 3).

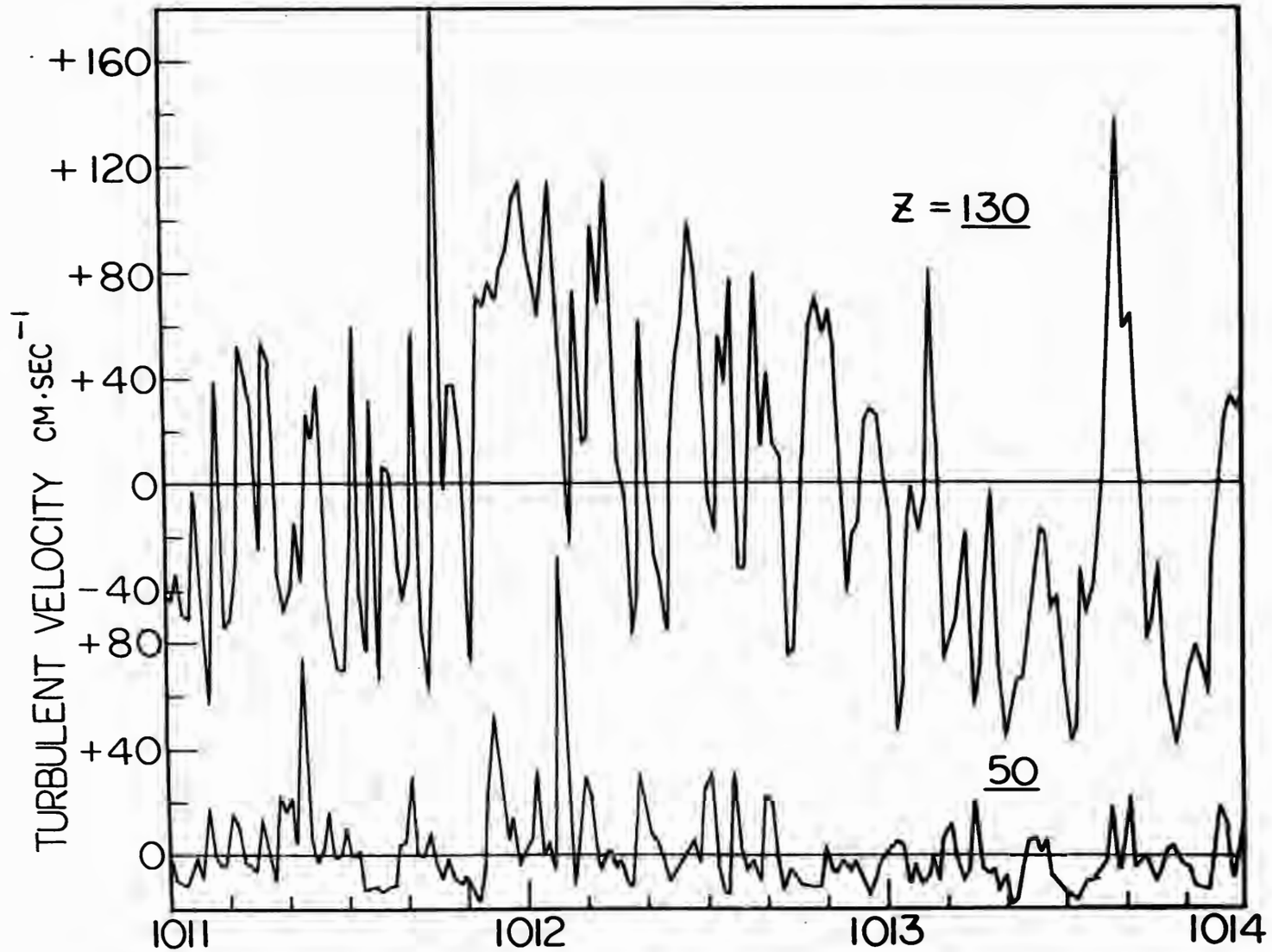

FIG. 14-B. WIND VELOCITY FLUCTUATION. (RUN 7).

At the lower wind velocity (Run 3), the upper levels of the plant-air layer display large unsteady wind fluctuations. On the contrary, at the higher wind velocity (Run 7), the fluctuation pattern between the upper and lower parts is quite the opposite. These results can be readily understood by comparing the values of the cross-correlation. At the lower wind velocity, the cross-correlation between the 130- and 50-cm. heights is 0.04, i.e., meaningless. At the higher wind velocity, the cross-correlation is about 0.3, seven times larger than for the lower wind velocity. From a comparison of the cross-correlation curves in and above the plant canopy (Run 3), it was found that in the plant-air layer the cross-correlation fell off rapidly, with pronounced assymmetry of the curve. This characteristic form ("cocked-hat") of the correlation curve agrees well with that for temperature fluctuations in a surface air-layer (Priestley, 1952). The assymmetric cross-correlation curve shows that the size of the wind fluctuations is relatively small; i.e., turbulent mixing is weak in the plant-air layer. Ogura, (1953) has given theoretical support for such a pronounced asymmetry in the cross-correlation curve of the surface air layer.

As an example of a wind fluctuation frequency distribution curve, Figure 15 clearly shows the change in the frequency distribution within the plant-air layer. As seen in Figure 15, the frequency distribution histograms show pronounced asymmetry, indicating a higher central peak and broader skirts than for a Gaussian function ($\mu_3 = 0.0$, $\mu_4 = 3.0$) of the same standard deviation.

In the investigation of the turbulent field behind turbulence grids placed in wind tunnels, the skewness, flatness, and intermittency factors frequently have been used to characterize some properties of turbulence (see Batchelor, 1953; Townsend, 1958). However, there are no experimental results for a surface air layer, particularly a plant-air layer, except those obtained by Inoue, Tani, Imai, (1957) and Gurvich, (1960). The three above mentioned

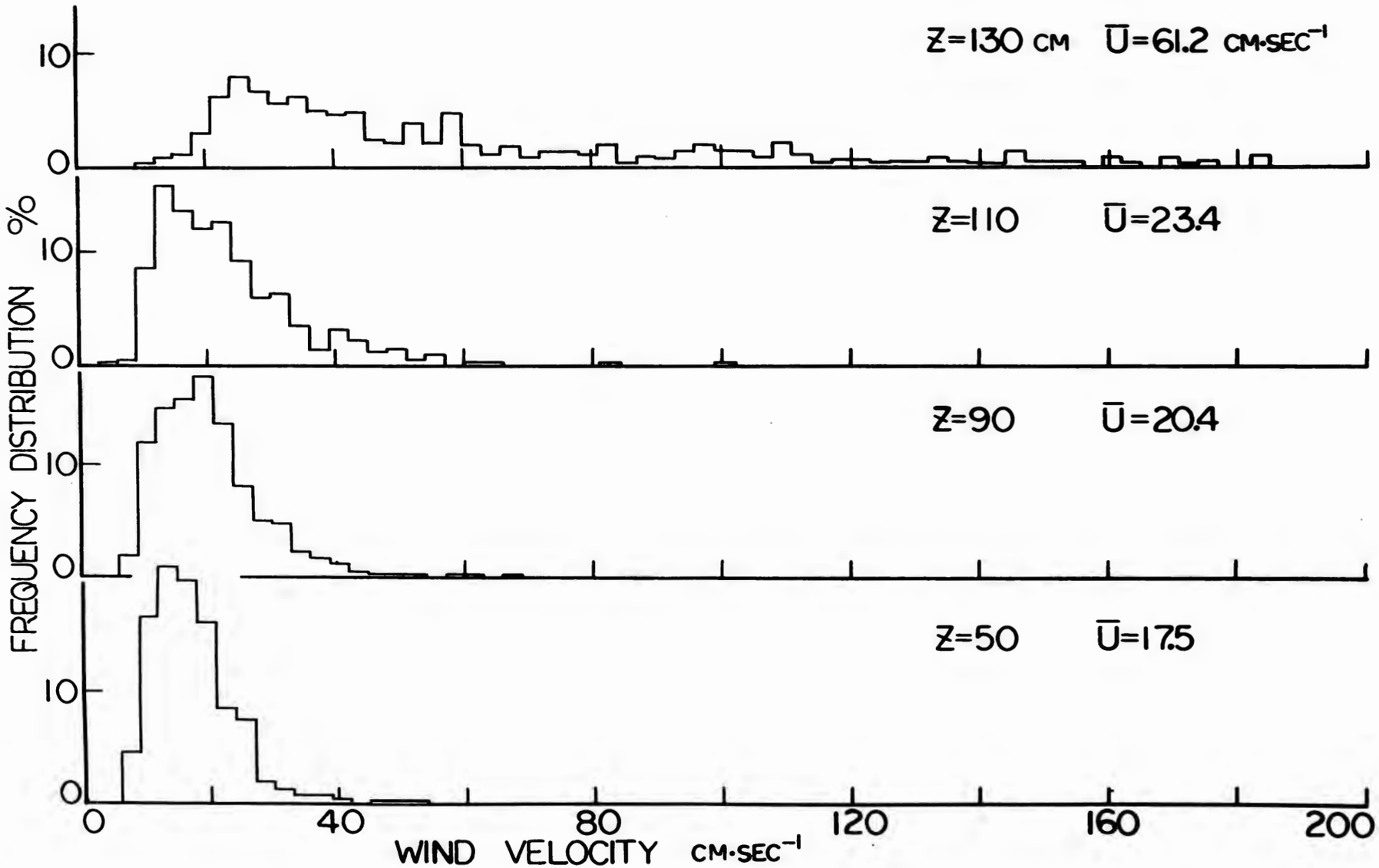

FIG. 15. FREQUENCY DISTRIBUTION OF WIND VELOCITY. (RUN 16)

factors are important in an investigation of the complicated nature of the turbulent field in plant-air layers. The skewness and flatness factors and the intermittency factor of the probability distribution of the wind velocity derivative ($\frac{du}{dt}$, t = 1 sec.) are presented in Table 4. In the surface air-layer at the lower wind speed (Run 3), the values of the skewness and flatness factors agree well with those (-0.3, 3.9) obtained by Batchelor and Townsend, (1949) for a turbulent field behind turbulence grids in a wind tunnel. Near the top surface of the plant-air layer, the skewness factor approaches zero. On the other hand, the flatness factor approaches 7.0, implying that both very small and very large values of $\frac{du}{dt}$ are more probable than in the case of normal distribution having the same standard deviation. For the lower part of the plant-air layer, the values of these factors are again close to those for a turbulent field behind a turbulent grid. On the other hand, at the higher wind velocity (Run 7), a very different vertical profile of these factors is observed in the plant-air layer. Namely, the probability density of the wind fluctuation near the top surface of the layer has values close to those for a turbulent field behind a grid, but at the lower levels it has larger skewness and flatness factors.

The nature of the probability density described above can easily be understood by introducing the effective intermittency, γ, which describes the proportion of the almost fully turbulent region to the whole region. At the lower wind velocity, the value of intermittency for the 370 and 50 cm. heights is in good agreement with that (γ = 0.78) for turbulent fields behind grids. However, the value near the top of the plant-air layer differs significantly from 0.78. At the higher wind velocity, the intermittency in the plant-air layer decreases from 0.68 near the top of the canopy to 0.20 at the 50 cm. height. The traces of the time derivative of wind velocity indicate that such small values of effective intermittency are caused by the

alternation between relatively quiet periods with low magnitudes of the derivative and active periods with large magnitudes. A comparison of the time traces of the wind velocity (u(t)) and of the time derivative of the wind velocity ($\frac{du}{dt}$) show that the active periods correspond to durations with high wind velocities.

5. SUMMARY

Meteorological research within vegetative canopies is an important field of agricultural research. The basic process of photosynthesis of organic matter depends upon the direct exchange of matter and energy between leaves and air within the plant-air layer. This exchange in turn, depends upon the air-flow characteristics of the vegetative canopy. Thus, air-flow characteristics, no less than the pattern of sunlight interception, form a vital part of the micrometeorology of photosynthesis.

In an investigation of air-flow within a corn crop, comprehensive measurements were made during the summer of 1962 at the Ellis Hollow cornfield of the USDA-Cornell University cooperative project. (This also was the major site of the field work on energy balance during 1960 and 1961.) Data obtained during the three days August 1 - 3 have been analyzed for momentum transfer and microstructure of turbulence within the height zone from the top of the corn to the ground.

The results may be summarized as follows:

(1) The wind profile within the canopy, normalized by the reference wind velocity $\bar{u}_H$ (z=H=140 cm. at the top of the crop), may be expressed as the sum of a logarithmic term and an additional term as follows:

$$\bar{u}_z = \bar{u}_H + A_0 \ln \frac{z}{H} + B_0 \cdot B'(z), \qquad z_0' \leq z \leq H.$$

The constants A_0 and B_0 were found to depend upon wind velocity, as follows:

$$A_0 = 0.25\ \bar{u}_H,$$

$$B_0 = 0.68\ \bar{u}_H.$$

The generalized function B'(z) represents the effect of the plant bodies on air flow. When the vertical distribution F(z) of aerial plant organs is taken as leaf area per unit volume of space (for corn, which is without branching stems), then B'(z) and F(z) have nearly similar shapes.

(2) Assuming a constant local drag coefficient, C, in the canopy, the momentum flux $\tau(z)$ was computed by,

$$\tau(z) = \tau_H - \rho C \int_z^H F(z) \overline{u_z^2}\, dz.$$

The vertical profiles of momentum flux and friction velocity were found to be approximately,

$$\tau(z) = \tau_H e^{-5.6\left(1-\frac{z}{H}\right)},$$

and

$$V_*(z) = V_{*H} e^{-2.8\left(1-\frac{z}{H}\right)},$$

where and

$$V_*(z) = \sqrt{\frac{\tau(z)}{\rho}} \qquad V_{*H} = \sqrt{\frac{\tau_H}{\rho}}.$$

(3) The exchange coefficient for momentum is assumed to be equal or nearly equal to the turbulent exchange coefficients for heat and matter (H_2O and CO_2 being of special interest) within the plant-air layer. The exchange coefficient was determined by the equation,

$$K(z) = \frac{\tau(z)}{\rho\left(\frac{d\bar{u}}{dz}\right)_z}.$$

Near the top of the crop, the exchange coefficient also decreased exponentially with depth into the canopy.

$$K(z) = K_H e^{-2.8\left(1-\frac{z}{H}\right)}.$$

The equation was valid over the height range, 60-140 cm. From the fitted equations for the vertical profile of the exchange coefficient, the diffusive resistance was computed by,

$$r_{z_1 \to z_2} = \int_{z_1}^{z_2} \frac{dz}{K(z)} .$$

The diffusive resistance for the whole plant-air layer ($z_1 = 0$, $z_2 = H$) was a hyberbolic function of wind speed, $\bar{u}_H$. The resistance $r_{z \to H}$ increased greatly with depth into the canopy (H-z).

(4) A mixing length for vertical turbulent transfers within the plant-air layer is given by,

$$l = \frac{V_*(z)}{\left(\frac{d\bar{u}}{dz}\right)_z} .$$

(This equation holds also for the constant-flux layer above plants.) Only at the heights of dense foliage (high F(z)) did the leaves limit the mixing length. Near the ground, the familiar equation,

$$l = \kappa (z + z_o')$$

was valid.

(5) The turbulent velocity (root-mean-square of the wind speed fluctuations) decreased exponentially with depth into the plant-air layer. In the top half of the canopy, ($\frac{H}{2} \leq z \leq H$), the relation was approximately,

$$\left(\overline{u'^2}\right)_z^{1/2} = \left(\overline{u'^2}\right)_H^{1/2} e^{-5.6\left(1 - \frac{z}{H}\right)} .$$

The turbulent velocity at any height varied as the square of the reference velocity $\bar{u}_H$. From this, it is assumed that the vertical profile of the turbulent velocity within the

layer is independent of wind velocity. For reference wind velocities between 36 and 170 cm/sec., the turbulent intensity at the 130 cm. height was in the range from 0.3 to 0.9. The turbulent intensity,

$$\frac{\sqrt{\overline{u'^2}}}{\overline{u}_z}$$

decreased gradually with depth (H-z).

(6) Wind speed fluctuation data were analyzed to specify the microstructure of turbulence in the plant-air layer. Since these measurements were time variations at a point, an equivalent separation distance, ℓ , was obtained from the lag time, σ , by $\ell = \bar{u} \cdot \sigma$. Among the quantities computed were the structure function, B_{dd}, structure parameter, B_v, energy spectrum, F(n), smallest eddy size, λ_2 , largest eddy size, Λ_{xo}, and kinetic energy dissipation rate, ϵ.

The spatial structure function for a turbulent field was defined by

$$B_{dd} = \overline{\left[u(x) - u(x+\ell)\right]^2} = 2\,\overline{u'^2}\left\{1 - R_u(\ell)\right\},$$

where $R(\ell)$ is the Eulerian space correlation.

It increased gradually with separation distance, $\ell = \bar{u} \cdot \sigma$. For small separation distances, the relationship was approximately

$$B_{dd} = B_v^{\,2} \cdot \ell^{2/3},$$

where B_v , the structure parameter, is proportional to the cube root of the dissipation rate, ϵ. The energy spectrum specifies the total turbulent energy as a function of frequency, n, by

(see over)

$$\frac{dE_T}{dn} = F(n) = 4\int_0^\infty R(\sigma)\cos(2\pi n\sigma)\,d\sigma,$$

where $R(\sigma)$ is the Eulerian time correlation.

The energy spectra obtained were more irregular than those for the surface air-layer, but in general the dependence of F(n) upon n was in good agreement with the negative 5/3 power law from the similarity theory. The ragged spectral curves seemed to result from disturbance of the air-flow caused by the waving and fluttering of corn leaves.

The smallest and largest eddy sizes, λ_2, and Λ_{x0}, mark the limits of the inertial subrange of turbulence, in which the familiar two-thirds and negative 5/3 power laws apply. They were evaluated by,

$$\lambda_2 = 15\left(\frac{\nu^3}{\epsilon}\right)^{1/4},$$

and

$$\Lambda_{x0} = \frac{1}{n^*}\,\bar{u}_z,$$

where,

ν = 0.14 $cm^2/sec.$ is the kinematic viscosity,

n^* is the frequency of the largest eddy of the inertial subrange,

$\bar{u}_z$ is the mean wind speed.

The value of λ_2 increased from 0.5 cm. at the top of the crop to 3.8 cm. at the 50 cm. height. The largest eddy Λ_{x0} showed less variation with height. The inertial subrange $(\Lambda_{x0} - \lambda_2)$ was of the order of 100 cm.

The turbulent energy dissipation rate was obtained from the structure parameter by the equation,

$$\epsilon = \frac{B_v^3}{(C_1)^3}.$$

In the upper part of the plant-air layer, the energy dissipation and structure parameter decreased exponentially with depth into the canopy. The equations

$$\epsilon = \frac{V_{*H}^3}{\ell(z)} e^{-8.4\left(1-\frac{z}{H}\right)},$$

$$B_T = \frac{C_1 \cdot V_{*H}}{[\ell(z)]^{1/3}} e^{-2.8\left(1-\frac{z}{H}\right)},$$

were applicable in the height range from 50 to 140 cm. The experimental results suggested that the similarity theory of turbulence can be applied to the plant-air layer. Some modifications of the concepts and defining equations that apply in the surface air layer (V_* , $\ell(z)$, etc.) are required before they can be correctly applied to the plant-air layer.

(7) To characterize experimentally the anisotropy of turbulence, both length and velocity coefficients of anisotropy were determined from the fluctuation data. They were defined by,

$$a_L = \frac{\ell_w}{\ell_u} \simeq \left\{ \frac{(\overline{u'^2})_c^{1/2}}{(\overline{u'^2})_m^{1/2}} \right\}^3,$$

$$a_V = \frac{\sigma_w}{\sigma_u} \simeq \frac{0.85 \cdot V_{*z}}{(\overline{u'^2})_z^{1/2}}$$

where $(\overline{u'^2})_c^{1/2}$ is the root-mean-square horizontal component velocity estimated by assuming isotropic condtions.

The eddy scale coefficient of anisotropy, a_L , showed a considerable decrease with increasing wind velocity, from

0.2 at 36 cm/sec. to 0.01 at 170 cm/sec. The turbulent velocity coefficient of anisotropy, α_L, also had wind velocity dependence. These results indicate that the turbulent field in the plant-air layer is anisotropic. Therefore, the vertical turbulent velocity $(\overline{w'^2})^{1/2}$ and vertical scale of eddy length, ℓ_w, cannot be replaced by their horizontal counterparts in determining the vertical exchange coefficient.

(8) The frequency distributions of the wind fluctuations within the plant-air layer were also analyzed. Measures of skewness and kurtosis were obtained from the third and fourth moments. The results showed the frequency curves to be non-Gaussian. Skewness and kurtosis varied with changes in the reference wind speed, $\bar{u}_H$, but differently at the top and at the bottom of the crop. In the upper part, these factors decreased moderately with increasing $\bar{u}_H$, but in the lower part they increased greatly. The time curves of turbulent velocity, u', and the time-derivative of wind velocity, $\frac{du}{dt}$ were compared. From this the above features were found to be a result of the penetration of high velocity gusts into the canopy. The cross-correlation between wind speed at the reference height z_R = 130 cm. and at other heights fell off rapidly with increasing separation $(z - z_R)$. This decrease was much greater in the downward than in the upward direction. This is another indication of the low intensity of turbulent mixing within the plant-air layer.

Acknowledgement

The authors wish to acknowledge the most helpful discussions and comments of E. R. Lemon, E. Inoue, and W. Covey in the preparation of this paper. The authors further wish to thank L. Hartwell Allen, Kirk W. Brown, Joseph H. Shinn, and Roger F. West for their generous help during the field experiments.

Finally, we extend thanks to W. Covey and L. Hartwell Allen for their critical reading of the text.

LITERATURE CITED

Batchelor, G. K. 1953. The Theory of Homogeneous Turbulence. Cambridge University Press. London. 197 p.

Baumgartner, A. 1956. Untershungen uber den Warme und Wasserhaushalt eines jungen Waldes. Ber. Deu. Aetterdienstes (5):1-53.

Broido, A. G. 1957. Some results of investigation on the integral exchange coefficient. [In Russian] Meteorol. i gidrol. (9):27-30.

Budyko, M. I. 1956. Heat Balance at Earth's Surface. [In Russian] Hydrometeorological Press. Leningrad. 280 p.

Fons, W. L. 1940. Influence of forest cover on wind velocity. J. Forest. 38:481-486.

Frenkiel, F. N. 1950. Frequency distributions of velocity in turbulent flow. J. Meteorol. 8:316-320.

Fritschen, L. J. and Shaw, R. H. 1961. A thermocouple-type anemometer and its use. Bull. Amer. Meteorol. Soc. 42:42-46.

Gifford, J. 1956. The relation between space and time correlations. J. Meteorol. 13:289-294.

Gurvich, A. S. 1960. Experimental study of frequency distribution of vertical velocity component in a surface air layer. [In Russian] Dok. Akad. Nauk USSR 132:806-809.

Imai, K. 1962. "Frequency distribution of velocity in a surface air layer." [Private communication]

Inoue, E. 1952. On the structure of wind near the ground. [In Japanese; English summary] Bull. Nat. Inst. Agr. Sci. A.2:1-93.

Inoue, Eiichi. 1963. The environment of plant surfaces, p. 23-31. In L. T. Evans, [ed], Environmental Control of Plant Growth. [Proceedings of Symposium, Canberra, Austr., August, 1962] Academic Press, New York and London.

Iwakiri, B. 1962. On the annual march of water temperature and heat balance items at shallow water. [In Japanese; English summary] J. Agr. Meteorol. Japan 17:133-138.

Kotoda, K. 1962. Some hydrometeorological characteristics of a paddy field. [In Japanese; English summary] J. Agr. Meteorol. Japan 17:151-159.

Lettau, H. 1949. Isotropic and non-isotropic turbulence in the atmospheric surface layer. Geophys. Research Paper (1):86.

MacCready, P. B. 1953. Atmospheric turbulence measurement and analysis. J. Meteorol. 10:325-337.

Medvedeva, G. P. 1962. External diffusion coefficient over ground surface and plant cover, p. 78-84. [In Russian] In . . . Heat Balance of Forest and Fields, Akad. Nauk Press, U.S.S.R.

Monteith, J. L. 1962. Gas exchange in plant communities, p. 95-111. In L. T. Evans, [ed], Environmental Control of Plant Growth. [Proceedings of Symposium, Canberra, Austr., August, 1962] Academic Press, New York and London.

Monin, A. S. 1958. On the structure of atmospheric turbulence. [In Russian] J. Theory of Stochastics and Its Application 3:285-305.

Monin, A. S. 1962. Empirical data on turbulence in the surface layer of the atmosphere. J. Geophys. Research 67:3106-3109.

Nakagawa, Y. 1956. Studies on the air flow amongst the stalks in a paddy field. [In Japanese; English summary] J. Agr. Meteor. Japan 16:61-63.

Obukhov, A. M. 1958. Rule of microstructure in temperature and wind velocity in the atmospheric surface layer, p. 131-137. [In Russian] In . . . Present Problems in the Study of the Atmospheric Surface Layer, Akad. Nauk Press, U.S.S.R.

Ogura, Y. 1952. Relation between the length of time under analysis and the statistical quantities of the atmospheric turbulence. J. Meteorol. Soc. Japan 30:103-111.

Ogura, Y. 1953. Note on the theory of turbulent diffusion in the lower layer of the atmosphere. J. Meteorol. Soc. Japan 31:125-131.

Panofsky, H. A. and Deland, R. J. 1959. One-dimensional spectra of atmospheric turbulence in the lowest 100 meters. Advances in Geophysics 6:41-64.

Penman, H. L. and Long, I. F. 1960. Weather in wheat: an essay in micro-meteorology. Quart. J. Roy. Meteorol. Soc. 86:16-49.

Perepelkina, A. V. 1957. Some results of investigation in turbulent fluctuations of temperature and vertical velocity component. [In Russian] Izv. Akad. Nauk Ser. Geofiz. (6):765-778.

Poppendieck, H. F. 1949. Investigation of velocity and temperature profiles in air layers within and above trees and brush. Sponsor, Office of Naval Research (Geophys. Br.) Contract N6-onr-275 Task Order VI Nr-082-036. University of California, Dept. of Engineering, Los Angeles. 45 p. (mimeographed).

Priestley, C. H. B. 1952. Atmospheric turbulence in the boundary layer. Geophys. Res. Paper (19):33-48.

Priestley, C. H. B. 1959. Turbulent Transfer in the Lower Atmosphere. University of Chicago Press, Chicago. 130 p.

Rauner, Iu. L. 1958. Some results of heat balance observations in a broadleaf forest. [In Russian] Izv. Akad. Nauk Ser. Geografi (5):79-86.

Rauner, Iu. L. 1960. Heat balance of forest. [In Russian] Izv. Akad. Nauk Ser. Geografi (1):49-59.

Saito, T. 1962. On estimation of transpiration and of eddy transfer coefficient within plant communities by energy balance method. [In Japanese; English summary] J. Agr. Meteorol. Japan 17:101-105.

Saito, T., Inoue, E., Isobe, S., and Horibe, Y. 1962. Heat exchange in a paddy field. [In Japanese; English summary] J. Agr. Meteorol. Japan 18:11-18.

Shiotani, M. 1953. Some notes on the structure of wind in the lowest layer of the atmosphere. J. Meteorol. Soc. Japan 31:327-335.

Shiotani, M. 1955. On the fluctuation of the temperature and turbulent structure near the ground. J. Meteorol. Soc. Japan 33:117-123.

Stoller, J. and Lemon, E. R. 1963. Turbulent transfer characteristics of the airstream in and above the vegetative canopies at the earth's surface, p. 34-46. In The Energy Budget at the Earth's Surface, Part II. U. S. Dept. of Agriculture Prod. Res. Report No. 72, U. S. Govt. Printing Office, Washington.

Tan, H. S., and Ling, S. C. 1963. A study of atmospheric turbulence and canopy flow, p. 31-27. In The Energy Budget at the Earth's Surface, Part II. U. S. Dept. of Agriculture Prod. Res. Report No. 72 U. S. Govt. Printing Office, Washington.

Taylor, R. J. 1952. Locally isotropic turbulence in the lower layers of the atmosphere. Geophys. Res. Paper (19):231-240.

Townsend, A. A. 1958. The Structure of Turbulent Shear Flow. Cambridge University Press, London. 315 p.

Uchijima, Z. 1959. An experimental study of the microstructure of turbulence over the warming pond. [In Japanese; English summary] Bull. Nat. Inst. Agr. Sci. A.7:101-130.

Uchijima, Z. 1961. On the characteristics of heat balance of water layer under paddy plant cover. Bull. Nat. Inst. Agr. Sci. A.8:243-265.

Uchijima, Z. 1962a. Studies on the microclimate within the plant communities (1) On the turbulent transfer coefficient within plant layer. [In Japanese; English summary] J. Agr. Meteorol. Japan 18:1-9.

Uchijima, Z. 1962b. Studies on the microclimate within the plant communities (2) The scale of turbulence and the momentum transfer within plant layers. [In Japanese; English summary] J. Agr. Meteorol. Japan 18:58-65.

Waterhouse, F. L. 1955. Micrometeorological profiles in grasscover in relation to biological problems. Quart. J. Roy. Meteorol. Soc. 81: 63-71.

Wright, J. L., and Lemon, E. R. 1962. Estimation of turbulent exchange within a corn crop canopy at Ellis Hollow, N. Y., 1961. Interim Report 62-7, USDA to USAR&D Activity, DA TASK 3A99-27-005-08, Cross Service Order 2-62, Ithaca, N. Y. 83 p. [Multilithed].

AD__________ Acession Nr.__________

Northeast Branch, Soil and Water Conservation Research Division, Agricultural Research Service, U. S. Department of Agriculture, Ithaca, N. Y.

AN EXPERIMENTAL STUDY OF AIR FLOW IN A CORN PLANT-AIR LAYER, by Zenbei Uchijima and James L. Wright.

Interim Report 63-1, July 1963, 75 pages, incl. illus., tables DA TASK 1-A-0-11001-B-021-08, Cross Service Order Nr. 2-63.

In an investigation of air-flow within a corn crop, data obtained have been analyzed for momen'um transfer and microstructure of turbulence. The data indicate that the height dependence of shearing stress, friction velocity, and exchange coefficient can be expressed as an exponential function of height. Results also indicate that the similarity theory of turbulence can be applied to the plant-air layer where divergence in momentum flux occurs. Also, the ragged nature of the spectral curve for the plant-air layer as compared to the surface air layer may be tentatively attributed to the waving and fluttering of plant leaves.

UNCLASSIFIED

1. Micrometeorology
2. Profiles
   Wind

UNCLASSIFIED

AD__________ Acession Nr.__________

Northeast Branch, Soil and Water Conservation Research Division, Agricultural Research Service, U. S. Department of Agriculture, Ithaca, N. Y.

AN EXPERIMENTAL STUDY OF AIR FLOW IN A CORN PLANT-AIR LAYER, by Zenbei Uchijima and James L. Wright.

Interim Report 63-1, July 1963, 75 pages, incl. illus., tables DA TASK 1-A-0-11001-B-021-08, Cross Service Order Nr. 2-63.

In an investigation of air-flow within a corn crop, data obtained have been analyzed for momentum transfer and microstructure of turbulence. The data indicate that the height dependence of shearing stress, friction velocity, and exchange coefficient can be expressed as an exponential function of height. Results also indicate that the similarity theory of turbulence can be applied to the plant-air layer where divergence in momentum flux occurs. Also, the ragged nature of the spectral curve for the plant-air layer as compared to the surface air layer may be tentatively attributed to the waving and fluttering of plant leaves.

UNCLASSIFIED

1. Micrometeorology
2. Profiles
   Wind

UNCLASSIFIED

AD__________ Acession Nr.__________

Northeast Branch, Soil and Water Conservation Research Division, Agricultural Research Service, U. S. Department of Agriculture, Ithaca, N. Y.

AN EXPERIMENTAL STUDY OF AIR FLOW IN A CORN PLANT-AIR LAYER, by Zenbei Uchijima and James L. Wright.

Interim Report 63-1, July 1963, 75 pages, incl. illus., tables DA TASK 1-A-0-11001-B-021-08, Cross Service Order Nr. 2-63.

In an investigation of air-flow within a corn crop, data obtained have been analyzed for momentum transfer and microstructure of turbulence. The data indicate that the height dependence of shearing stress, friction velocity, and exchange coefficient can be expressed as an exponential function of height. Results also indicate that the similarity theory of turbulence can be applied to the plant-air layer where divergence in momentum flux occurs. Also, the ragged nature of the spectral curve for the plant-air layer as compared to the surface air layer may be tentatively attributed to the waving and fluttering of plant leaves.

UNCLASSIFIED

1. Micrometeorology
2. Profiles
   Wind

UNCLASSIFIED

AD__________ Acession Nr.__________

Northeast Branch, Soil and Water Conservation Research Division, Agricultural Research Service, U. S. Department of Agriculture, Ithaca, N. Y.

AN EXPERIMENTAL STUDY OF AIR FLOW IN A CORN PLANT-AIR LAYER, by Zenbei Uchijima and James L. Wright.

Interim Report 63-1, July 1963, 75 pages, incl. illus., tables DA TASK 1-A-0-11001-B-021-08, Cross Service Order Nr. 2-63.

In an investigation of air-flow within a corn crop, data obtained have been analyzed for momentum transfer and microstructure of turbulence. The data indicate that the height dependence of shearing stress, friction velocity, and exchange coefficient can be expressed as an exponential function of height. Results also indicate that the similarity theory of turbulence can be applied to the plant-air layer where divergence in momentum flux occurs. Also, the ragged nature of the spectral curve for the plant-air layer as compared to the surface air layer may be tentatively attributed to the waving and fluttering of plant leaves.

UNCLASSIFIED

1. Micrometeorology
2. Profiles
   Wind

UNCLASSIFIED

UNCLASSIFIED